Report No. 6140
Copy No.

UNDERWATER VIEWING SYSTEM USING SOUND HOLOGRAPHY

Final Technical Report

April 1972

Research Sponsored By:

Office of Naval Research
Washington, D.C.

Contract N000 14-68-C-0338
NR 261-170/6-26-70 (466)

The Bendix Corporation
Research Laboratories
Southfield, Michigan 48076

76
R

Unclassified
Security Classification

DOCUMENT CONTROL DATA - R&D

(Security classification of title, body of abstract and indexing annotation must be entered when the overall report is classified)

1. ORIGINATING ACTIVITY (Corporate author) Bendix Research Laboratory Bendix Center Southfield, Michigan 48076	2a REPORT SECURITY CLASSIFICATION 2b GROUP

3. REPORT TITLE

Underwater Viewing System Using Sound Holography (U)

4. DESCRIPTIVE NOTES (Type of report and inclusive dates)

Final Technical Report — 1 May 1968-31 January 1972

5. AUTHOR(S) (Last name, first name, initial)

P. N. Keating, R. Koppelmann and R. F. Steinberg

6. REPORT DATE	7a TOTAL NO. OF PAGES	7b. NO OF REFS
March 1972		

8a. CONTRACT OR GRANT NO.	9a. ORIGINATOR'S REPORT NUMBER(S)
N00014-68-C-0338 b. PROJECT NO. c. d.	6140 9b OTHER REPORT NO(S) (Any other numbers that may be assigned this report)

10. AVAILABILITY/LIMITATION NOTICES

11. SUPPLEMENTARY NOTES	12. SPONSORING MILITARY ACTIVITY
Details of illustrations in this document may be better studied on microfiche	Office of Naval Research Washington, D.C.

13. ABSTRACT

A feasibility study and prototype system development for an underwater viewing system based on acoustic holographic principles was initiated at Bendix Research Laboratories in 1968 under contract #N00014-68-C-0338. The objective was to study various receiving array configurations and construct a modular prototype system to evaluate the capabilities of holographic concepts. In parallel, the development of a system for real-time optical reconstruction of sampled holograms was initiated.

This report presents a summary of the program activities from its inception in 1968 to its completion in 1971. Accomplishments include completion of the design and construction of the underwater viewing system as well as that for the coherent light area modulator. Experimental verification of the system's operational capabilities was also completed. This includes the generation of holograms using the underwater viewing system and various target configurations, and the reconstruction of these holograms using the coherent light area modulator.

The results of an analysis of synthetic and nonplanar holographic arrays are additionally included in this report.

DD FORM 1 JAN 64 1473

Unclassified
Security Classification

Unclassified
Security Classification

14. KEY WORDS	LINK A		LINK B		LINK C	
	ROLE	WT	ROLE	WT	ROLE	WT
Underwater Viewing						
Acoustic Holography						
Coherent Light Area Modulator						
Real Time Holographic Reconstruction						
KDP Modulator Tube						
Conformal Arrays						
Synthetic Apertures						

INSTRUCTIONS

1. ORIGINATING ACTIVITY: Enter the name and address of the contractor, subcontractor, grantee, Department of Defense activity or other organization *(corporate author)* issuing the report.

2a. REPORT SECURITY CLASSIFICATION: Enter the overall security classification of the report. Indicate whether "Restricted Data" is included. Marking is to be in accordance with appropriate security regulations.

2b. GROUP: Automatic downgrading is specified in DoD Directive 5200.10 and Armed Forces Industrial Manual. Enter the group number. Also, when applicable, show that optional markings have been used for Group 3 and Group 4 as authorized.

3. REPORT TITLE: Enter the complete report title in all capital letters. Titles in all cases should be unclassified. If a meaningful title cannot be selected without classification, show title classification in all capitals in parenthesis immediately following the title.

4. DESCRIPTIVE NOTES: If appropriate, enter the type of report, e.g., interim, progress, summary, annual, or final. Give the inclusive dates when a specific reporting period is covered.

5. AUTHOR(S): Enter the name(s) of author(s) as shown on or in the report. Enter last name, first name, middle initial. If military, show rank and branch of service. The name of the principal author is an absolute minimum requirement.

6. REPORT DATE: Enter the date of the report as day, month, year, or month, year. If more than one date appears on the report, use date of publication.

7a. TOTAL NUMBER OF PAGES: The total page count should follow normal pagination procedures, i.e., enter the number of pages containing information.

7b. NUMBER OF REFERENCES: Enter the total number of references cited in the report.

8a. CONTRACT OR GRANT NUMBER: If appropriate, enter the applicable number of the contract or grant under which the report was written.

8b, 8c, & 8d. PROJECT NUMBER: Enter the appropriate military department identification, such as project number, subproject number, system numbers, task number, etc.

9a. ORIGINATOR'S REPORT NUMBER(S): Enter the official report number by which the document will be identified and controlled by the originating activity. This number must be unique to this report.

9b. OTHER REPORT NUMBER(S): If the report has been assigned any other report numbers *(either by the originator or by the sponsor)*, also enter this number(s).

10. AVAILABILITY/LIMITATION NOTICES: Enter any limitations on further dissemination of the report, other than those imposed by security classification, using standard statements such as:

(1) "Qualified requesters may obtain copies of this report from DDC."

(2) "Foreign announcement and dissemination of this report by DDC is not authorized."

(3) "U. S. Government agencies may obtain copies of this report directly from DDC. Other qualified DDC users shall request through _____."

(4) "U. S. military agencies may obtain copies of this report directly from DDC. Other qualified users shall request through _____."

(5) "All distribution of this report is controlled. Qualified DDC users shall request through _____."

If the report has been furnished to the Office of Technical Services, Department of Commerce, for sale to the public, indicate this fact and enter the price, if known.

11. SUPPLEMENTARY NOTES: Use for additional explanatory notes.

12. SPONSORING MILITARY ACTIVITY: Enter the name of the departmental project office or laboratory sponsoring *(paying for)* the research and development. Include address.

13 ABSTRACT: Enter an abstract giving a brief and factual summary of the document indicative of the report, even though it may also appear elsewhere in the body of the technical report. If additional space is required, a continuation sheet shall be attached.

It is highly desirable that the abstract of classified reports be unclassified. Each paragraph of the abstract shall end with an indication of the military security classification of the information in the paragraph, represented as *(TS)*, *(S)*, *(C)*, or *(U)*.

There is no limitation on the length of the abstract. However, the suggested length is from 150 to 225 words.

14. KEY WORDS: Key words are technically meaningful terms or short phrases that characterize a report and may be used as index entries for cataloging the report. Key words must be selected so that no security classification is required. Identifiers, such as equipment model designation, trade name, military project code name, geographic location, may be used as key words but will be followed by an indication of technical context. The assignment of links, rules, and weights is optional.

Unclassified
Security Classification

Report No. 6140

UNDERWATER VIEWING SYSTEM USING SOUND HOLOGRAPHY

Final Technical Report

April 1972

Research Sponsored By:

Office of Naval Research
Washington, D.C.

Contract N000 14-68-C-0338
NR 261-170/6-26-70 (466)

The Bendix Corporation
Research Laboratories
Southfield, Michigan 48076

ABSTRACT

A feasibility study and prototype system development for an underwater viewing system based on acoustic holographic principles was initiated at Bendix Reseach Laboratories in 1968 under contract #N00014-C-68-0338. The objective was to study various receiving array configurations and construct a modular prototype system to evaluate the capabilities of holographic concepts. In parallel, the development of a system for real-time optical reconstruction of sampled holograms was initiated.

This report presents a summary of the program activities from its inception in 1968 to its completion in 1971. Accomplishments include completion of the design and construction of the underwater viewing system as well as that for the coherent light area modulator. Experimental verification of the system's operational capabilities was also completed. This includes the generation of holograms using the underwater viewing system and various target configurations, and the reconstruction of these holograms using the coherent light area modulator.

The results of an analysis of synthetic and nonplanar holographic arrays are additionally included in this report.

TABLE OF CONTENTS

LIST OF ILLUSTRATIONS

SECTION 1
SUMMARY

1.1 GENERAL

Advances in sound holography had, by 1968, demonstrated the feasibility of undertaking a program to develop a real-time underwater viewing system based on holographic principles. Such a system offers advantages over conventional oceanographic search and surveillance techniques, such as optical viewing and sonar. Optical viewing is limited to relatively short ranges under turbid water conditions, and sonar is limited in its ability to provide detailed target information. Acoustic holography on the other hand provides an imaging system which is relatively unaffected by water turbulence and turbidity, and which will produce images over a relatively large field of view. Therefore, in 1968, Bendix Research Laboratories, under the auspices of the Office of Naval Research, undertook the task of developing an experimental viewing system based on holographic principles.

The design of the underwater viewing system was based on what would be required for a shipboard operational system. A modular approach, however, was taken in the construction of the prototype model. The advantages of this approach were that a smaller, less costly development program was needed, and the complete system operation could be entirely determined by the operation and performance of the prototype.

1.2 VIEWING SYSTEM

The viewing system (consisting of an acoustic projector, a 20 x 20 receive array, and signal processing electronics) samples the output of each element of the receive array and generates the holographic data for all elements. The data, when displayed in their entirety, make up a hologram of the acoustic field appearing across the face of the receive array during the sample period.

Considerations affecting the choice of an operating frequency included array dimension, seawater attenuation of acoustic energy, and frequency dependent noise considerations.

The range was chosen to bridge the gap between optical viewing and sonar. Optical viewing is only useful at very short ranges, depending on water conditions. Sonar is limited by the difficulty in interpreting the return signal in terms of specific identifiable objects. At long ranges (greater than 100 meters), sonar would be useful for initially locating possible objects. At intermediate ranges, the acoustic imaging system would present a more definitive picture of the object to the operator, and at distances less than 2 meters, direct optical viewing would be optimum.

For most applications, an angular resolution of 0.4 degree (for a 100 x 100 array) and a viewing angle of 40 degrees appear sufficient. This angular resolution results in lateral resolution of 4 inches (10 cm) at 50 feet (~15 meters). The lateral resolution is naturally better at shorter ranges and worse at longer ranges since the angular resolution

is essentially constant. Since the resolution is related to the total aperture size, and the development effort here was to use the modular approach (i.e., build a 20 x 20 element array rather than a 100 x 100 array in order to reduce costs), the angular resolution of the prototype system is limited to 2 degrees.

The viewing system is operated in a pulsed rather than a CW mode for several reasons. These include the capability of imaging moving targets, interrogating specific range increments, using smaller transmitting elements for a given peak radiation power (by using a small duty cycle), and discriminating against unwanted reflections from surfaces beyond the range being interrogated.

The design and construction of the underwater viewing system were successfully completed in 1970 and a demonstration for the representatives of the Office of Naval Research, Naval Ships, and NUWC was given in July of that year.

1.3 IMAGE DISPLAY TUBE

A parallel effort to develop a coherent light area modulator for real-time optical reconstruction of holograms was also initiated at Bendix Research Laboratories in 1968.

The conventional method of using photographic film as the recording medium for holograms requires the development of the film for reconstruction, and therefore does not leand itself to a real-time system. Since the underwater viewing system requires a method for reconstructing holograms in real time, the development of the coherent

light modulator was of particular importance to the success of the overall effort.

The heart of the coherent light modulator is a DKDP crystal which exhibits the property of field-induced birefringence. When the modulator is operating in the transmissive mode, the coherent light will, as it passes through the crystal, experience phase modulation proportional to the field applied to the crystal. Reconstruction of a hologram is therefore accomplished by using an electron gun, whose beam is modulated by the holographic data obtained from the underwater viewing system, to establish a field across the DKDP crystal which is proportional to the acoustic field sensed by the acoustic array. Since the field applied to the DKDP is, in effect, a hologram corresponding to the diffraction pattern on the acoustic array, the diffracted laser beam, when focused by an optical lens, gives a reconstructed real-time image of the object in the acoustic field.

Construction of the coherent light area modulator was completed in 1971 and an initial demonstration was given for representatives of the Department of Naval Research.

1.4 SYSTEM TESTING

Various tests using the coherent light area modulator and the underwater viewing system were performed to verify the system's operational capabilities.

The real-time capability of the reconstructor tube was demonstrated by moving a static hologram while reconstructing the image. The

electronics for the reconstructor tube were designed to operate at 30 frames per second; however, since the tube must go through an erase, write, and view cycle for each reconstruction, the operational frame rate is limited to 10 frames per second.

The field of view and resolution capabilities of the underwater viewing system were verified using three closely spaced targets. Holograms of the three targets were made and the reconstructed image was used for the above verification. The apparent spreading of the images provided a measure of the system's resolution capabilities while the location of the first-order diffraction pattern in the reconstructed image was used to verify the system's viewing angle.

The system's capability to image moving targets was also tested. Two types of effects were noted: one is the familiar Doppler effect, while the other is image blurring due to lateral motion. The test results demonstrated that the system is capable of imaging moving targets which display up to 30 knots of Doppler. Additionally, the system is also capable of imaging laterally moving targets with velocities up to 150 knots.

1.5 CONFORMAL ARRAYS

An analysis of conformal arrays and the implementation of such arrays with respect to applications in operational holographic systems was performed as part of the overall program effort. The analysis shows that by applying the proper phase compensation to the received signals, effective conformal arrays can be implemented. A study of the

methods for introducing this phase compensation indicate that the most promising approach is the use of a small digital computer. The most promising analog method is to introduce positional shifts to various parts of the hologram which upon reconstruction would have the effect of introducing the required phase shifts.

1.6 REPORT SUMMARY

The following report is divided into four main sections consisting of

- The underwater viewing system
- The coherent light area modulator
- Experimental test results using the above systems
- An analysis of synthetic and nonplanar arrays with respect to applications in holographic systems

Previous reports have covered portions of the developmental program in detail. Therefore, certain sections of the following report only summarize what has been previously reported and will cite the reports which are pertinent to that section.

SECTION 2

DESIGN OF THE UNDERWATER VIEWING SYSTEM

2.1 GENERAL

The underwater viewing system is made up of an acoustic section and an electronics section. The acoustic section consists of (i) a projector used to insonify the viewing area and (ii) a 20 x 20 receive array used to detect any returning signals reflected by targets in the insonified area.

The electronic system consists of (i) 400 parallel signal processing channels, each of which is asscciated with a particular element within the receive array and generates the holographic data for that element, (ii) a multiplexing section which sequentially samples the stored data and routes these data in a serial fashion to a display CRT or to the reconstructor, and (iii) a timing section which controls the sequence of events for the entire system.

In the remainder of this section, the design specifications and considerations are discussed, and the major system components are described.

2.2 DESIGN SPECIFICATIONS AND CONSIDERATIONS

The design specifications for the prototype underwater viewing system were detailed and discussed in the original Bendix Proposal No. 4353 to ONR. These specifications are summarized below.

Operating Frequency:	250 kHz
Range:	Up to 100 meters
Angular Resolution:	0.4 Degree
Viewing Angle:	40 Degrees

The system should also be capable of detecting and imaging target objects with a speed relative to the system of at least 10 knots.

2.3 ACOUSTIC PROJECTOR

The acoustic projector is composed of a spherical shell of piezoelectric ceramic vibrating in a radial mode. A spherical configuration was chosen to give the maximum transmitting surface area and radiation resistance. The high radiation resistance and the relatively low stiffness of the shell give a low mechanical "Q" which in turn gives wide bandwidth and good transient response. The piezoelectric material is a barium titanate composition, CH 300. This material has a high sound velocity; thus the resonant sphere has a large enough diameter so that it can be manufactured without special tooling and excessive costs. For the particular application of this mission, a mechanical Q of 6 has been realized with maximum power limited by cavitation (5 watts in the pulsed mode). The unidirectional radiation pattern of the single sphere is shown in Figure 2-1.

2.4 RECEIVE ARRAY

The receive array is composed of lead zirconate titanate slugs mounted to form a planar square in an acoustically soft baffle. The elements are placed 1.5 wavelengths apart so that the proper viewing aperture is achieved. It is noted that uniformity of element response (amplitude and phase detection) is of paramount importance. For this reason, 6-8 db sensitivity was sacrificed and nonresonant elements were used.

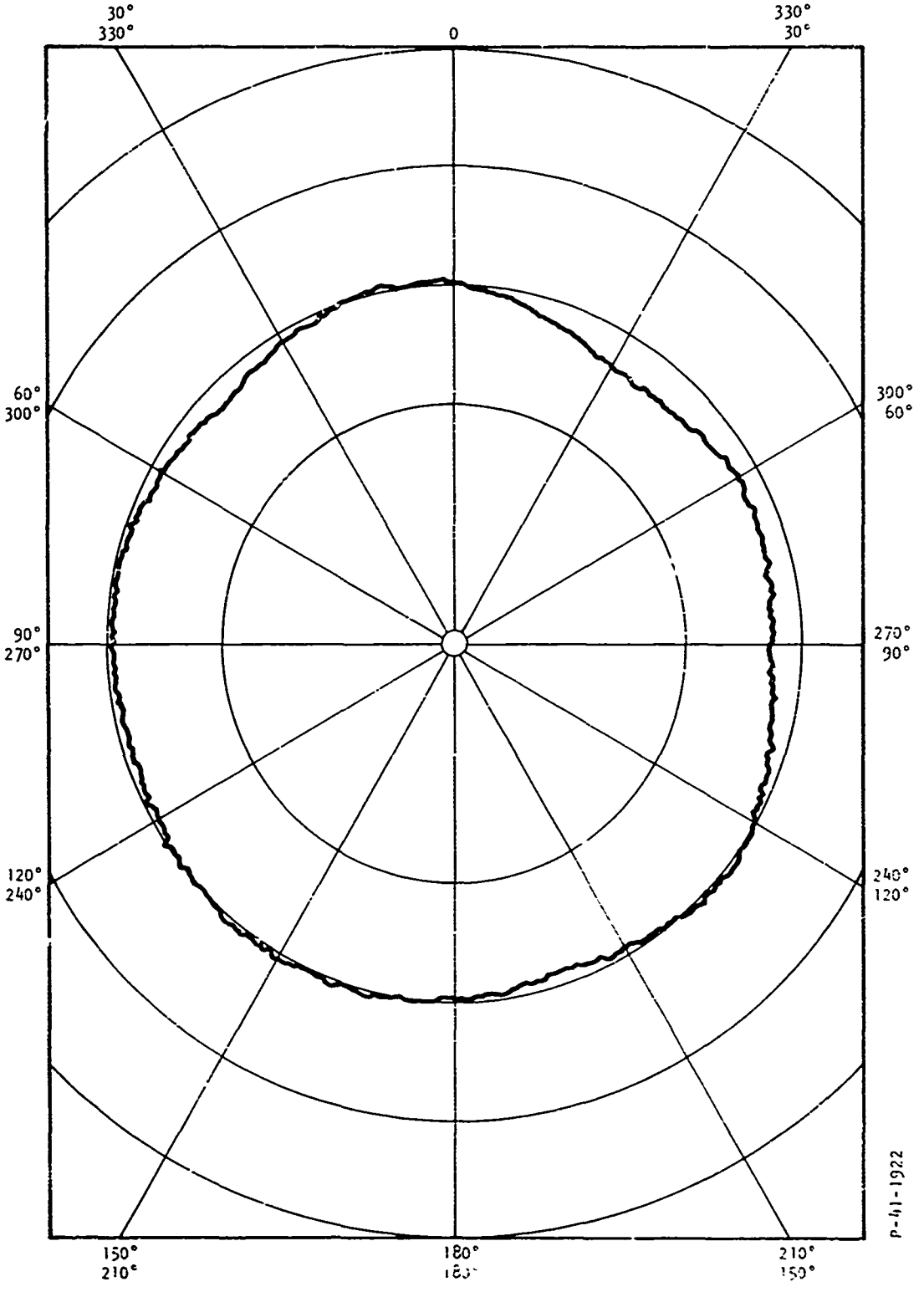

Figure 2-1 - Radiation Pattern of a Single Sphere (With No Absorber)

It was extremely important to provide a good acoustic baffle for each element, so that each would be as close as possible to an isotropic radiator. At the same time, their diameter was made close to a wavelength (for high sensitivity), and they were spaced only 1.50 wavelengths from each other (to provide a wide response over $\pm$20 degrees). A lead-corprene baffled system was finally chosen, while the hydrophones themselves were manufactured from Gulton G-1512 material. Their sensitivity was better than -105 db ref 1V/μbar (at the operating frequency, far below resonance). The measured detectability pattern (equivalent to radiation pattern) of such an arrangement is plotted in Figure 2-2. It is observed that the acoustic response is almost constant (within 3 db) in the forward sector. Thus, spurious and unwanted reflections will not interfere with the target information. Figure 2-2 shows a typical detectability pattern for a single element within the array.

The assembled array is shown in Figure 2-3. The housing in back of the array contains the electronic boards that generate the holographic signal.

2.5 ELECTRONIC SYSTEM

This section describes the signal processing portion of the system which generates electronically, on a point-by-point basis, the holographic data. A simplified block diagram of the overall system is shown in Figure 2-4.

The signal is received from each linear element of the acoustic array, mixed with a reference signal, averaged (integrated) for a pre-

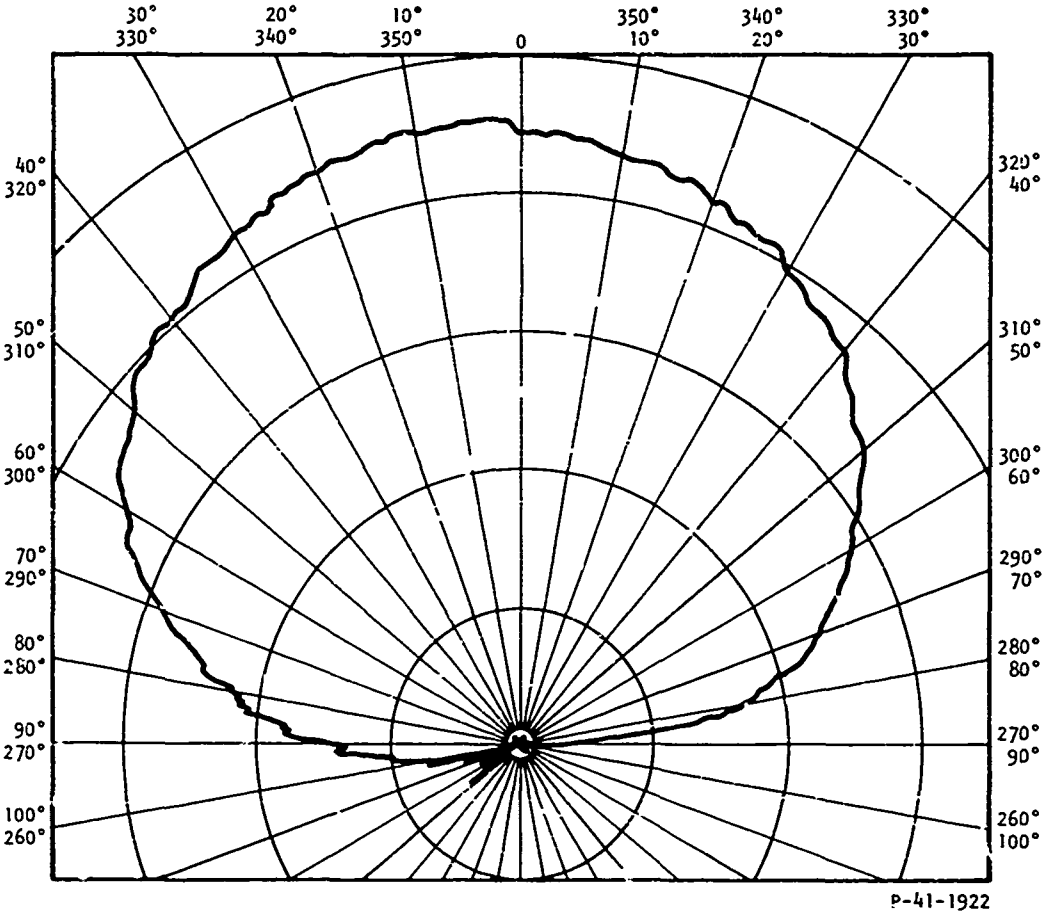

Figure 2-2 - Detectability Pattern of a Typical Element of the Receiver Array (Figure 2-3)

determined length of time, and finally stored as a constant (DC) level. This constant level, proportional to both the amplitude and the cosine of the phase of the detected signal, represents the local holographic information which, when displayed for all points, makes up a complete hologram.

The reference signal, when considered for all points of the receive array, must simulate a plane wave whose angle of incidence with the array is variable. This inclined reference plane wave is simulated using

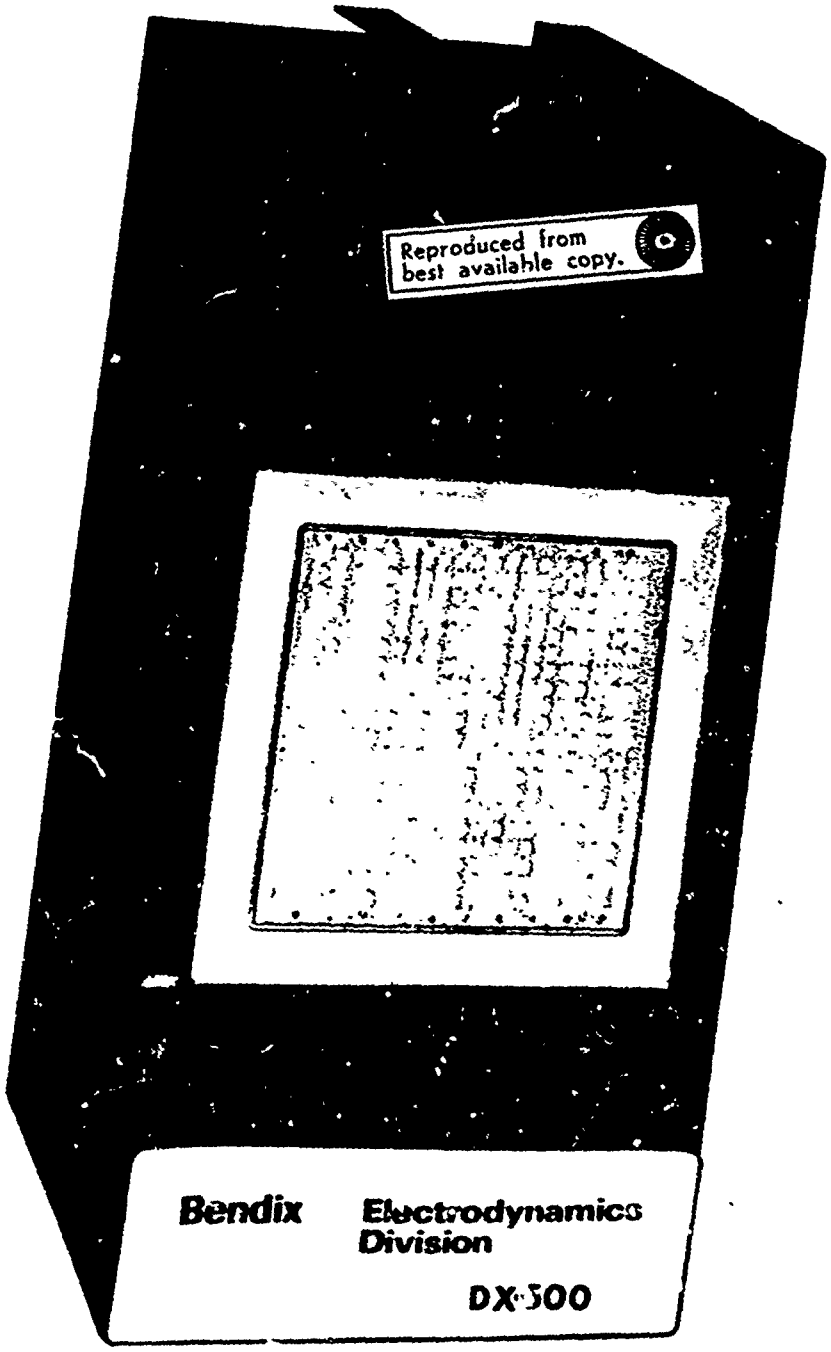

Figure 2-3 - Receive Array with Housing

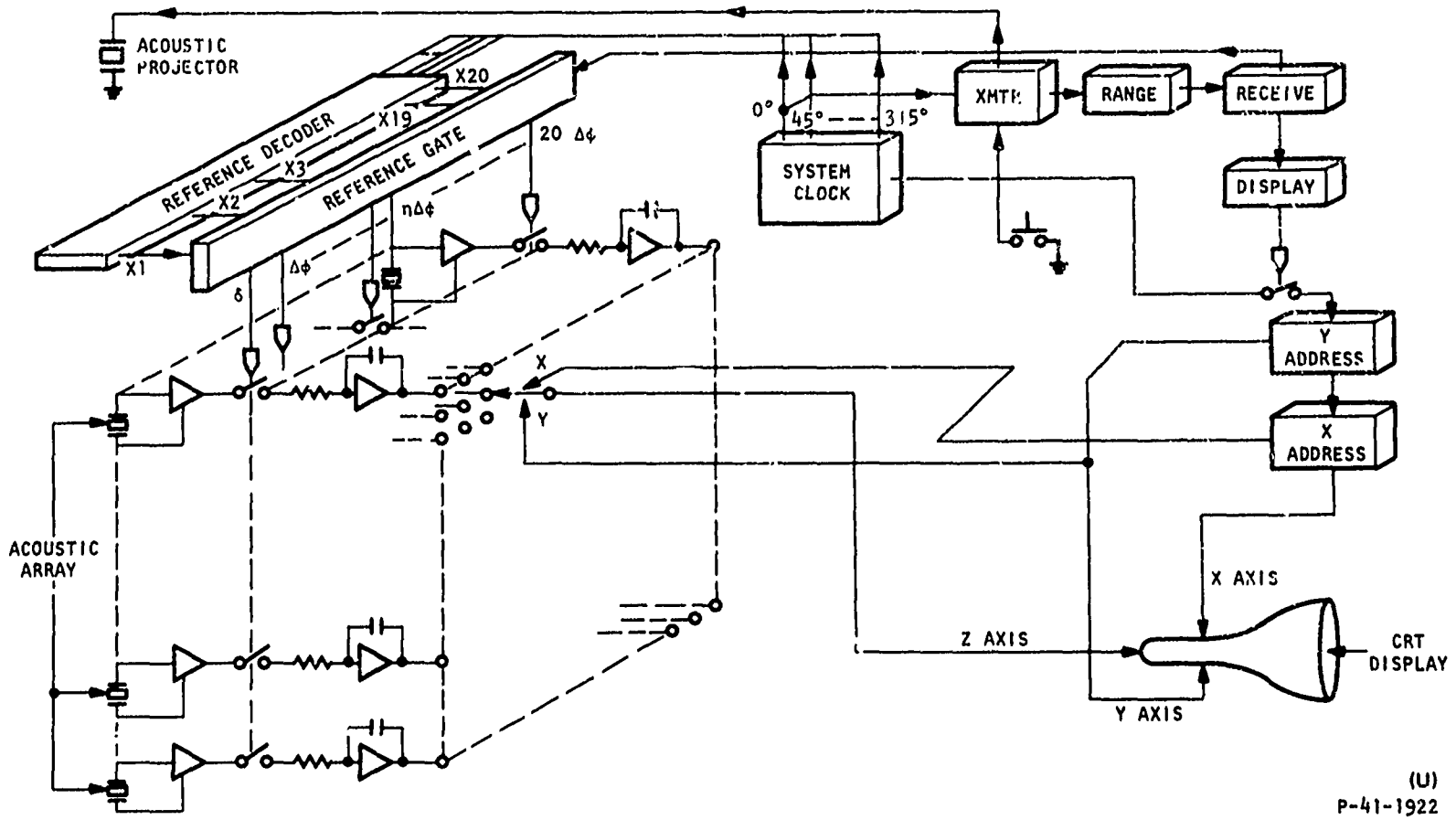

Figure 2-4 - Block Diagram of UVS System

several reference signals applied to different parts of the array, each of which is shifted in phase from the previous signal by a fixed amount. During the receive mode of operation, each column of signal processing channels receives a reference signal that is incremented in phase with respect to the previous column. Thus the reference plane wave is simulated, with an apparent angle of incidence determined by the phase increment between adjacent columns.

The sequence of events for a single system cycle is initiated by depressing the SINGLE TRANSMIT button. This triggers the transmit multivibrator which gates the drive signal to the transmitter. The range multivibrator, which provides a system delay equal to the two-way propagation of the transmitted wavefront, is also triggered at this time.

After the range delay, the system goes into a receive mode. In this mode, the simulated reference is gated to the signal processing circuitry where it is multiplied with the incoming signal. For each element, the product of this multiplication is integrated and stored as a DC level.

The receive mode is followed by a display mode, during which the system sequentially samples the stored DC levels and displays the information in the form of a dot matrix on a cathode ray tube which was used for experimental testing of the system. Through the use of a common clock, the readout address is synchronized to ensure that the CRT display has the same X-Y address as the information being sampled. The intensity of each dot corresponds to the value of the sampled DC level. Since each DC level is proportional to the local holographic information,

the display of the 400 DC levels is the desired hologram. A photograph of this hologram provides a permanent record from which a transparency can be made; an optical reconstruction can be made by conventional techniques.

The processing circuitry associated with each element generates the holographic signal $K_m \cos(\phi_m - \phi_r)$ for that point. Figure 2-5 shows a simplified schematic of the circuitry.

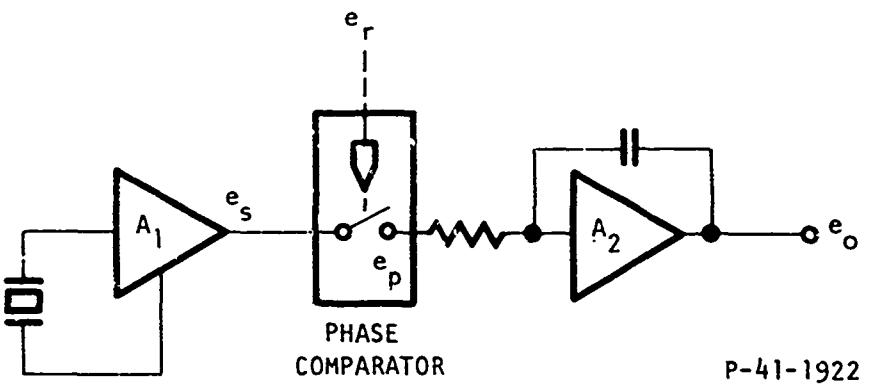

Figure 2-5 - Single-Channel Processing Circuitry

The input to amplifier A_1 can be expressed as $K_m(\omega t + \phi_m)$, where ω is the frequency of the sound, and ϕ_m is the phase of the signal at the m-th channel.

During the receive period, this signal is multiplied with the internally-generated reference signal, which in our case is a square wave:

$$e_r = \frac{1}{2} + \frac{2}{\pi}\cos(\omega t + \phi_r) - \frac{2}{3}\cos(3\omega t + 3\phi_r) + \ldots$$

The multiplier is an electronic switch which performs a phase comparison of the two signals. The output of the phase comparator contains a term $A_1 K_m/\pi \{\cos (\phi_m - \phi_r)\}$ proportional to the phase difference between the two signals, as well as other terms fluctuating at high rates (ω, 2ω, etc.).

The amplifier A_2 following the phase comparator, and its associated circuitry, form an integrator which rejects the signal harmonics and integrates the DC component (frequency independent) to provide a signal

$$\frac{A_1 A_2 K_m}{\pi} T_r \cos (\phi_m - \phi_r)$$

where T_r is the receive time. At the end of the receive command, the phase comparator switch opens and the integrator "holds" the final signal for display. This phase comparator-integrator combination determines the system bandwidth as $1/2\ T_r$.

A more detailed detailed description of the electronics section is contained in report No. 5362 submitted to the Office of Naval Research December 1970.

SECTION 3
REAL TIME HOLOGRAPHIC RECONSTRUCTION TUBE

3.1 GENERAL

The development of that part of the Underwater Viewing System (UVS) described in Section 2 (acoustic projector, receive array, processing and display electronics) made it possible to generate and display an acoustic hologram representative of the object field. To make the system complete, however, a device capable of converting this holographic information into a visual image, in real-time, was required. The development of such a device was started during the initial portion of this contract on a cost-shared basis (ONR and Bendix). Further development was continued throughout the contract period in a parallel program funded by Bendix.

3.2 DESIGN SPECIFICATIONS

Initial specifications were chosen to meet a set of illustrative mission requirements. It was not intended that these be fixed criteria, nor was it intended that they represent the maximum potential of an operational system. The specifications were chosen on the basis of what appears to be practical now in terms of "typical" mission requirements, complexity, cost, and development time. The total system specifications establish the minimum performance criteria for the reconstructor (display) device and reduce to the following:

1. The electrical signals from the detectors comprising the receive array must be made to modulate (phase or amplitude)

a beam of coherent light, while preserving the relative positions of the detectors and phase of the signals in the modulation pattern.

2. The resolution must be sufficient to resolve 100 x 100 or 10^4 elements.
3. The time required to establish and remove the modulation must be short enough to permit the presentation of 10 frames per second.

Other requirements such as image brightness, physical size, weight, etc., are important but were not believed to be as critical as the above three with respect to demonstrating the feasibility of producing a usable device.

3.3 DESIGN CONSIDERATIONS

A number of possible approaches to modulating light with the speed and resolution necessary were considered. Some of those which appeared most feasible involve the use of electro-optical materials, photochromic materials, liquid crystals, and deflecting membranes. However, all the approaches which can have holographic applications, and for which the most successful operating imaging devices have been reported, involve the use of electro-optical materials. Consequently, it appeared best to pursue the use of electro-optical materials at least for the initial stage of the program. The possibility of using the other approaches listed above was reviewed throughout the development period, but the choice of electro-optical materials still appears to be the best.

The electro-optical materials selected for use in the development of a real-time reconstructor device was KD_2PO_4 (DKDP). This material was chosen as the one best satisfying the following desirable material properties:

1. A relatively large linear electro-optic effect.
2. Low optical absorption at the wavelengths of the various lasers which may be used for reconstruction.
3. High resistivity
4. Optical uniformity, so that light passing through the material does not lose coherence
5. Good mechanical strength and chemical stability
6. The electro-optical effect for light rays parallel to the electric field should be linear and as large as possible in at least one crystal direction.
7. The material should be relatively hard and rigid.

Other design considerations, such as the choice of a sweeping electron beam to place a charge-pattern corresponding to the hologram on the surface of the electro-optical crystal, were discussed in detail in the "First Interim Report," Bendix Report No. 4601, dated August 1968.[1]

3.4 DESCRIPTION AND OPERATION OF REAL TIME RECONSTRUCTOR DEVICE

The reconstructor device were described in detail in the First Interim Report, Bendix Report No. 4601. Since that report, the tube has been modified in order to obtain better performance and to achieve a real time display capability. Because of these modifications, the design, operation, and characteristics of the present reconstructor

assembly will be reviewed here. Much of the following discussion was reported in a paper, "Real-Time Optical Reconstruction and Display of Acoustic Holograms for an Underwater Viewing System,"[2] presented at the Electro-Optics '71 East Conference in September 1971. Addition detail, particularily relating to tube life and reliability, was included in the "Interim Report," (Bendix Report No. 5406)[3] submitted in January 1971.

3.4.1 Reconstructor and Design

Basically, the reconstructor consists of a thin, z-cut, deuterated KH_2PO_4 (DKDP) crystal, an off-axis scanning electron gun, and the associated optics and electronic controls. The DKDP is 1/2 to 1/4 mm thick and optically flat over the center (20 mm by 20 mm) area. It is cemented onto a CaF_2 crystal which provides a transparent mechanical support and an isothermal surface. A transparent conducting gold film is deposited on the side of the DKDP in contact with the CaF_2. The other side is coated with a thin film which protects the DKDP from damage by the scanning electron beam. A grid (crystal grid) is located close to the DKDP to collect secondary electrons during writing and return them to the crystal during erasing. This structure is shown schematically in Figure 3-1.

3.4.2 Principle of Operation

In the normal mode of operation, the gold film is grounded, and the scanning electron beam is modulated with the holographic information. Because the crystal grid is positive and the secondary yield

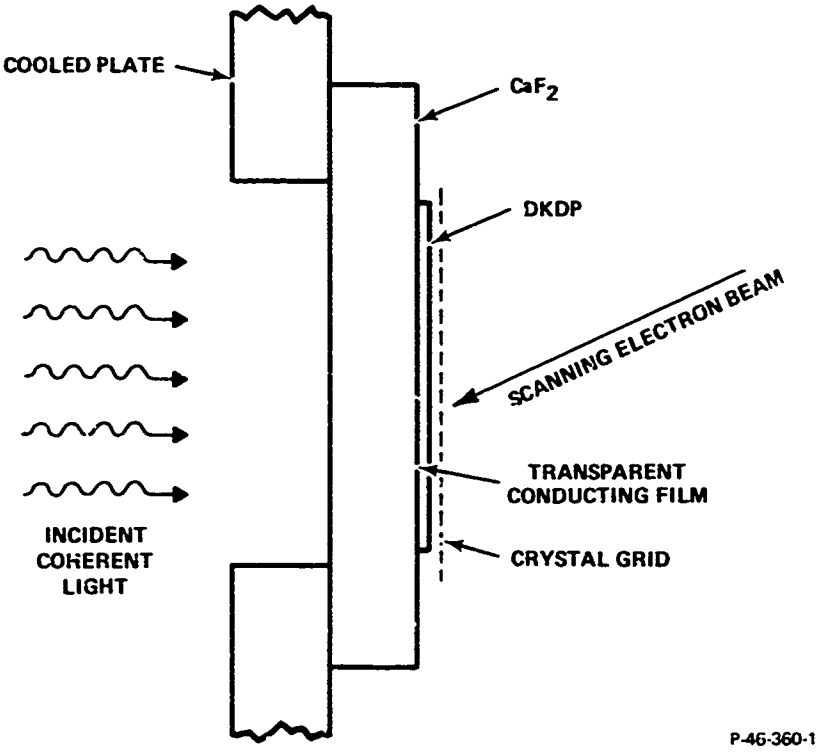

Figure 3-1 - DKDP Crystal and Mounting

is greater than one, a hologram is written on the DKDP in the form of a positive charge pattern. The resulting electric field between these charges and the grounded Au film (i.e., within the DKDP) varies over the crystal according to the holographic signal. Because DKDP has a large longitudinal electro-optic coefficient, the refractive index is thereby modulated, and coherent-light transmitted through the DKDP crystal becomes phase-modulated with the holographic information. The hologram is erased by scanning the DKDP with a constant electron beam while the crystal grid is at a small negative potential.

Because of the nature of the electro-optic effect, the transmitted light is phase-modulated. However, if the light incident

on the DKDP is linearly polarized along one of the crystal axes, and a crossed (at a 90 degree angle) analyzer is positioned on the other side of the crystal, the light transmitted through the analyzer will then be amplitude-modulated. The total light transmitted will vary as $\sin^2 KV(x,y)$ where $V(x,y)$ is the voltage across the thickness of the crystal at any point on the surface. A number of imaging devices which utilize a DKDP crystal in this manner have been reported; however, this is the first application of this type of a device to holographic reconstruction.

3.4.3 DC Light Filtering

One very important result of applying this modulator to holography is that it is possible to greatly reduce background noise due to the DC light. This happens automatically with the use of a crossed analyzer. It can be shown[4] that when the incident light is polarized along a crystal axis, the even-order diffraction (including the zero-order DC) will be polarized in the same direction and the odd-order diffractions will be rotated 90 degrees. Consequently, a crossed analyzer will block the DC (and any higher even-order) and pass the image light which is the first-order diffraction. For maximum effectiveness of this technique, the average charge on the crystal should be near zero. This can be achieved by a suitable choice of the crystal grid potential during the erase cycle.

3.4.4 Crystal Temperature

The DKDP crystal is cooled during operation. In the development of the prototype device, this was accomplished by flowing

cold N_2 gas through a heat exchanger in the tube; future models would use thermoelectric coolers. There are three reasons for cooling the crystal: first, to obtain useful light modulation with smaller crystal voltages; second, to increase the resolution; and third, to decrease the crystal conductivity.

3.4.4.1 Phase Modulation

When the crystal is cooled towards the Curie temperature (T_c), the dielectric constant for fields along the c-axis (ε_c) increases. This is illustrated by the data of Busch shown in Figure 3-2. Here, both ε_c and ε_c (which equal ε_b, and is the dielectric constant along the c-axis) are shown as a function of temperature for KDP. While ε_a is almost independent of temperature above T_c, ε_c varies as $(T-T_c)^{-1}$. The results are similar for deuterated KDP except that the Curie point is raised to about -50°C. The electro-optical coefficient (r_{63}), which determines the voltage required for a given amount of light modulation, is proportional to $(\varepsilon_c-\varepsilon_a)$. Therefore, the voltage needed for useful modulation can be reduced by well over a factor of ten by cooling the crystal.

3.4.4.2 Resolution

The second reason for cooling the DKDP is that the resolution is improved. It can be shown[4] that the resolution (in terms of resolvable line pairs/cm), when limited by field spreading within the DKDP, varies as $(\varepsilon_c/\varepsilon_a)^{1/2}$ and, therefore, as $(T-T_c)^{-1/2}$. The results of an experimental test of the relationship between resolution

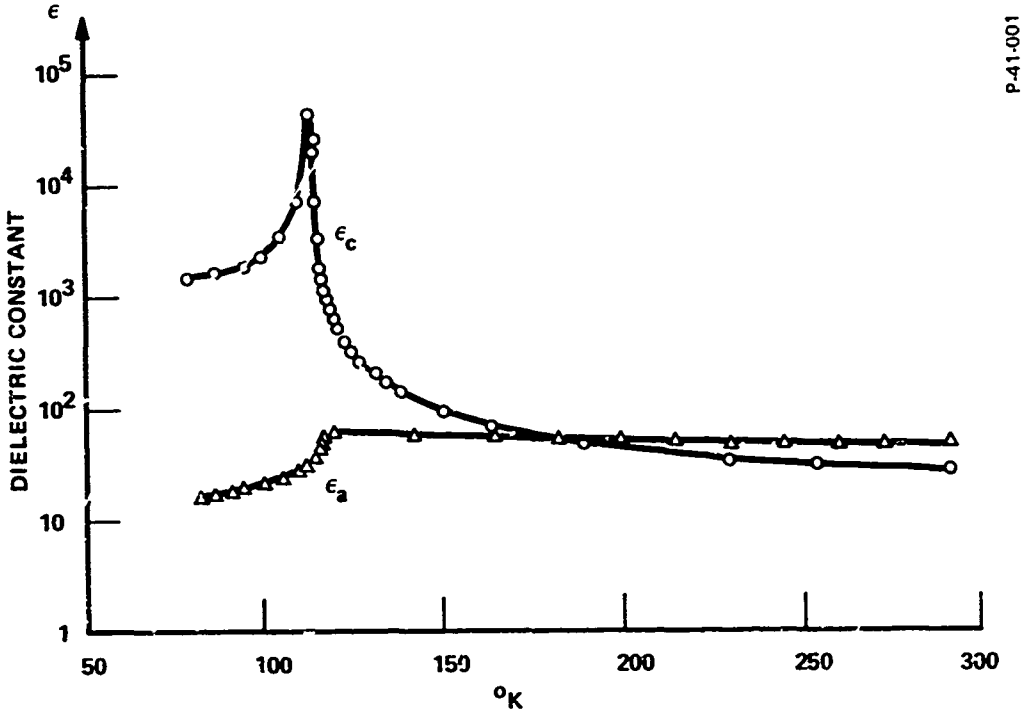

Figure 3-2 - Dielectric Constants ϵ_c and ϵ_a of KH_2PO_4, Measured at 800 cps with a Signal of 200 volts/cm (after Busch)

and temperature is shown in Figure 3-3. Here the limiting resolution in line pairs/cm was determined at several temperatures and plotted as a function of $(T-T_c)^{-1/2}$. At the higher temperatures, the measurements agree with the predicted relationship. Near the Curie temperature, the resolution was determined by the spot size of the electron beam, and not by field spreading; hence the deviation from the linear relationship. Since the useful area of the DKDP crystal is 2 x 2 cm^2, the data indicate that the modulator can resolve approximately 300 lines, or 9 x 10^4 points. Since this exceeds the requirements for the underwater viewing system, no attempt has been made to increase it. However, if required,

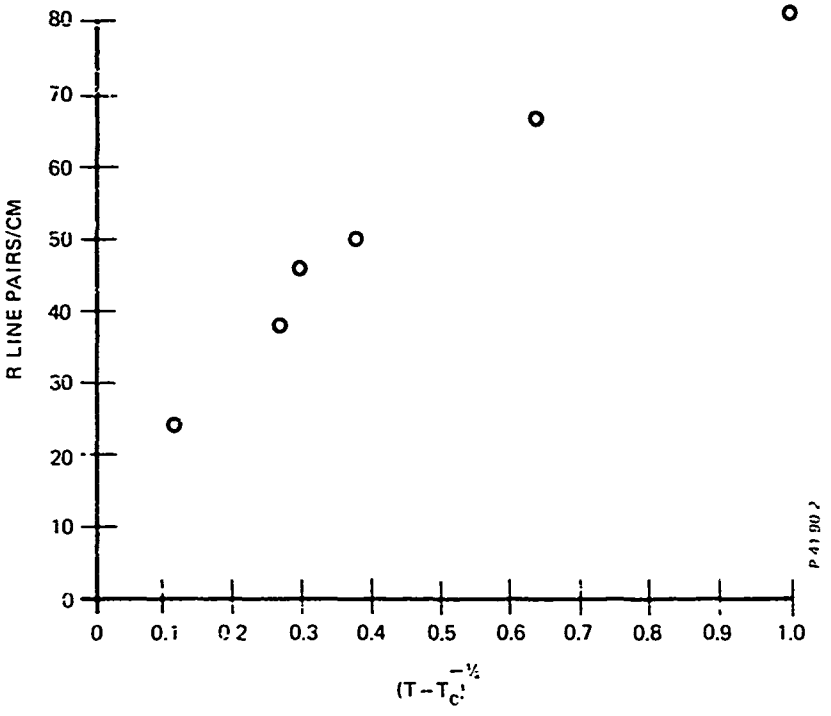

Figure 3-3 - Dependence of the Resolution R Upon Function $(T - T_c)^{-1/2}$

a larger area crystal or a thinner crystal combined with a higher resolution electron gun can be used to increase the information capacity.

3.4.4.3 Crystal Conductivity

The third reason for cooling is to reduce the conductivity of the DKDP. At room temperature, the dielectric relaxation time (the time constant for charge leakage through the crystal to the Au film) is of the order of 0.1 sec but can vary as much as an order of magnitude. Moreover, part of the conduction is ionic, and this transfer of ions can degrade the modulator. By cooling the DKDP to below -15°C and operating the tube so that the average charge on the crystal is near zero, both of these problems can be essentially eliminated.

Operating temperatures below -15°C are also desirable because of better resolution and larger electro-optic modulation. However, temperatures lower than T_c + 4°c are rarely used, because of stresses which can occur at temperatures very close to T_c.

3.4.5 Modulator Electronics

The modulator electronics are designed to accept two types of holographic video information. The first type of video signal conforms to the standard television format in that the composite signal contains the vertical and horizontal sync information as well as the video information. The second type of holographic information consists of a video signal only, while the vertical and horizontal sync information is contained in sweeps which are generated external to the electronics unit. This flexibility allows the use of a TV camera for experimental work and also leaves the unit compatible with the Bendix underwater viewing system which generates the horizontal and vertical sweep voltages in addition to the video signal. A block diagram of the electronics unit is shown in Figure 3-4.

The optical reconstructor must go through a three-step sequence (erase, write, and view) to reconstruct a particular hologram. The vertical sync or trailing edge of the vertical sweep provides the timing for this sequence. The sequence for reconstructing a hologram starts with the receipt of the first video frame, during which time the electron gun acts as a flood gun and erases any charge stored on the reconstructor crystal. The second sync signal cycles the reconstructor

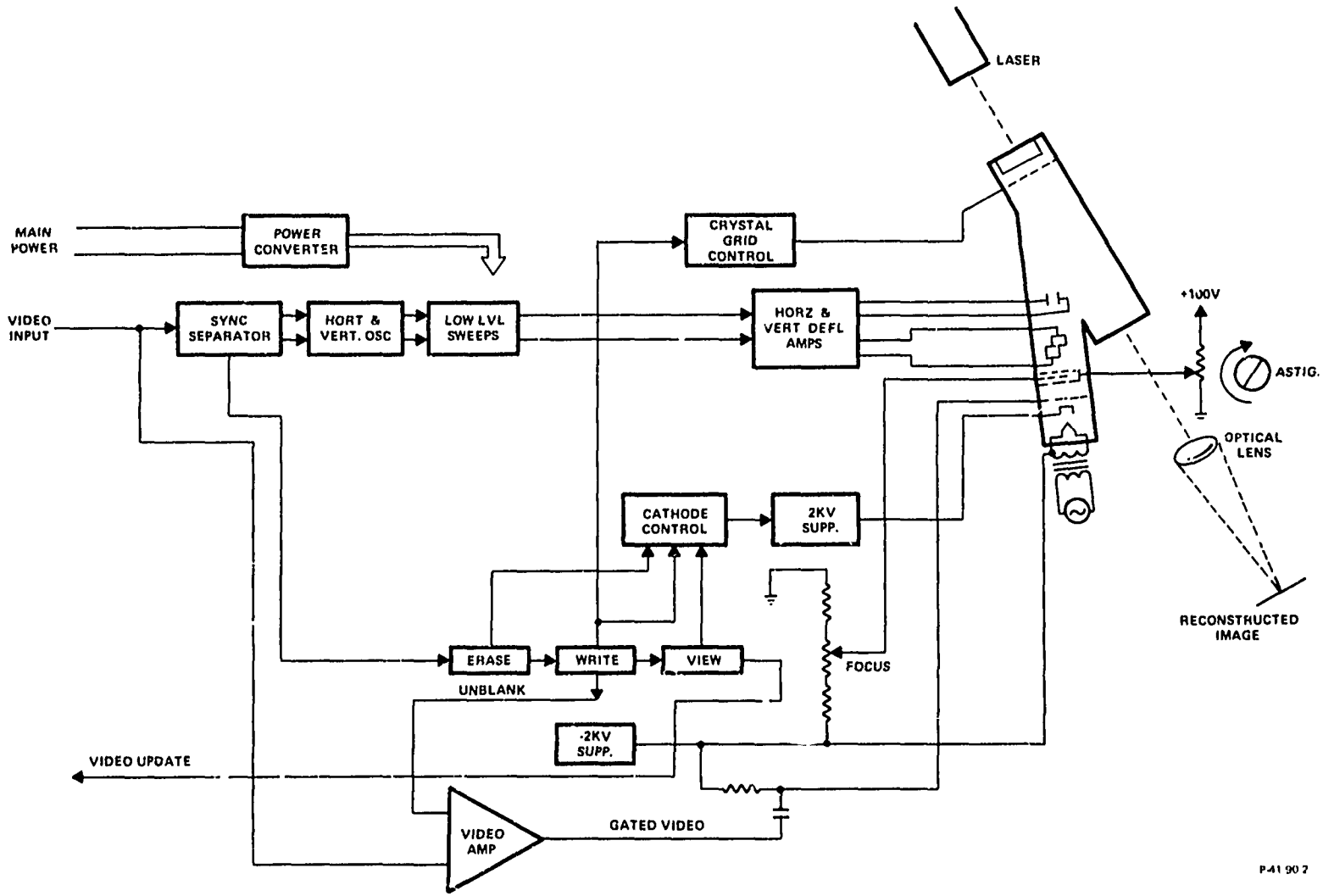

Figure 3-4 - Electronics Unit Block Diagram

into the write mode, during which time the new video information is written on the reconstructor crystal. The third sync signal will cycle the reconstructor into a view mode during which time the coherent light source is gated on and reconstruction of the hologram takes place. If the reconstructor is mated with the underwater viewing system, it will, then generate a video update command which initiates a new transmit, range, receive, and display cycle for the viewing system.

Referring to the electronics unit block diagram, the unit is divided into two main sections:

- The sweep circuits
- The electron gun control circuits

3.4.5.1 Sweep Circuits

The sweep circuits consist of sync separation circuitry followed by a vertical and horizontal oscillator and two low level sweep generators. The sync separation and oscillator circuits are standard circuits which employ off the shelf IC's in their design. The low level sweep circuits generate a voltage ramp which sweeps from 0V to 1V. The externally generated sweep is a 0-to-1V digital ramp; therefore, the remainder of the sweep circuitry is common to both inputs.

The sweep ramps are fed to the horizontal and vertical deflection amplifiers which provide the voltage gain required to drive the electron gun deflection plates.

3.4.5.2 Electron Gun Control Circuit

The control circuits consist of a cathode control circuit and a crystal grid control circuit. The cathode control circuitry

is used to control the cathode-to-grid voltage for the erase-write-view sequence. Since the electron gun is in the cut-off region during the view cycle, which can be as long as 10 seconds, a DC coupled control is best suited for this application. This is presently accomplished by using a 2kV supply for DC coupling and then modulating the low voltage side of the supply.

The crystal grid control circuit is used to obtain an average charge near zero on the crystal over one erase-write-view cycle. It consists of an electronic switch which switches the crystal grid to a positive voltage during the write period and to a small negative voltage during the erase period.

The above sequences are initiated by T^2L logic which is used to keep track of the frame count and to synchronously step the electronics unit through the erase-write-view cycle.

3.5 OPERATIONAL TESTS

Development of the two subsystems, the real-time reconstructor (light modulator) and the receive array and signal processing subassembly, was carried out in parallel programs, and the operational testing was done in two separate locations. Hence, the modulator was tested using simulated time-varying acoustical holograms. In the tests, prints of static holograms were viewed with a vidicon TV camera as they were oscillated through an angle of 45 degrees. Thus, the video signals from the camera represented a time-changing hologram. These signals were used to operate the reconstructor and produce images which changed position with time. Examples of reconstructions obtained in real-time

operation, together with the acoustical holograms which produced them, are shown in Figures 3-5 and 3-6. Video tapes of the reconstruction of these holograms, and of another higher resolution hologram, were also made to demonstrate and document the real-time capability of the reconstructor.

The maximum operation rate possible with the present electronics is 10 frames (complete cycles including erase, write, and view) per second. However, for easy viewing of more complex objects, it is necessary to increase the writing time to accumulate more charge on the crystal. This in turn reduces the frame rate. For example, the reconstruction in Figure 3-5 was obtained at an operation rate of 10 frames per second and that in Figure 3-6 at a rate of 5 frames per second. Alternatively, the use of a more sensitive TV monitor camera or an image intensifier eliminates the need to reduce the frame rate for complex images.

3.6 LIFE AND RELIABILITY

Life and reliability in earlier image tubes using KDP crystals were limited by such problems as: (a) the crystal can crack for a variety of reasons, (b) its surface can be damaged by the electron bombardment, and (c) outgassing from the crystal assembly can poison the electron gun cathode or even cause the tube to become gassy. Much of the development effort was therefore directed toward solving such problems. A variety of cements were tested for better compatibility with the DKDP and better vacuum characteristics. Several different protecting films have been evaluated for resistance to electron-bombardment-induced damage, color center formation, and decrease in secondary

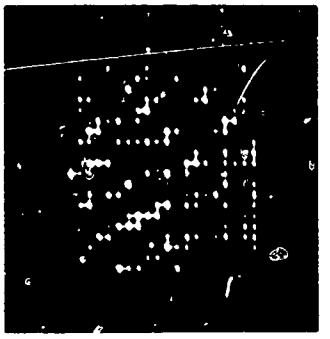

(a) – Underwater Acoustic Holograms of 3 Discs Taken by 20 x 20 Transducer Array

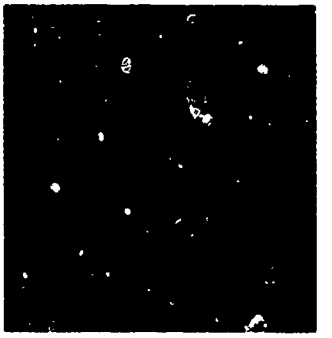

(b) – Reconstruction with DKDP Light Modulator

Figure 3-5 - Underwater Acoustic Hologram and Its Reconstruction

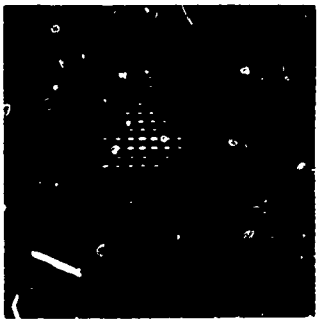

(a) – Acoustic Hologram of Letter E, Taken by Scanning Transducer

(b) – Real-Time Reconstruction with DKDP Light Modulator

Figure 3-6 - Acoustic Hologram and Its Reconstruction

yield. Safe operating limits for the voltage across the DKDP at various temperatures have been established. As a result of these studies, the life and reliability of the device have now been greatly improved. The current tube, which has an attached ion pump, has been operational for a half year without any problems. Tests have shown the useful life of the present protecting film to be well in excess of 1000 hours under continuous bombardment with a longer total operating time likely for intermittent operation. Consequently, even though some further improvements are likely, particularly in the protective film, the modulator can be considered a practical device at the present time.

SECTION 4
EXPERIMENTAL TESTING

4.1 UNDERWATER VIEWING SYSTEM

4.1.1 Static Tests

Testing of the underwater viewing system using three stationary targets has been previously reported.[3] However, due to misalignment of the targets, the results were less than satisfactory. Therefore, a similar experiment was performed using three square targets measuring 76 mm (3 inches) on the side. The targets were first individually placed and holograms were made; then all three targets were placed and a hologram of the combination was recorded. Figure 4-1 shows the placem of the three targets, and Figure 4-2 shows the placement of the underwater viewing system. A dimensional layout of the targets with respect to the receive array is shown in Figure 4-3.

The holograms were optically reconstructed and are shown in Figures 4-4, 4-5, 4-6, and 4-7 which correspond to targets #1, #2, #3, and the combination of all three, respectively.

Referring to Figure 4-7, the bright spot in the center of the photograph is due to the zero-order light which consists of an out-of-focus D.C. spot and a convolution term. To the right of the zero-order light is the first repeat of the zero-order pattern (first-order diffraction pattern) at a lower intensity. This repeated pattern is due to the discrete nature of the underwater array and corresponds to

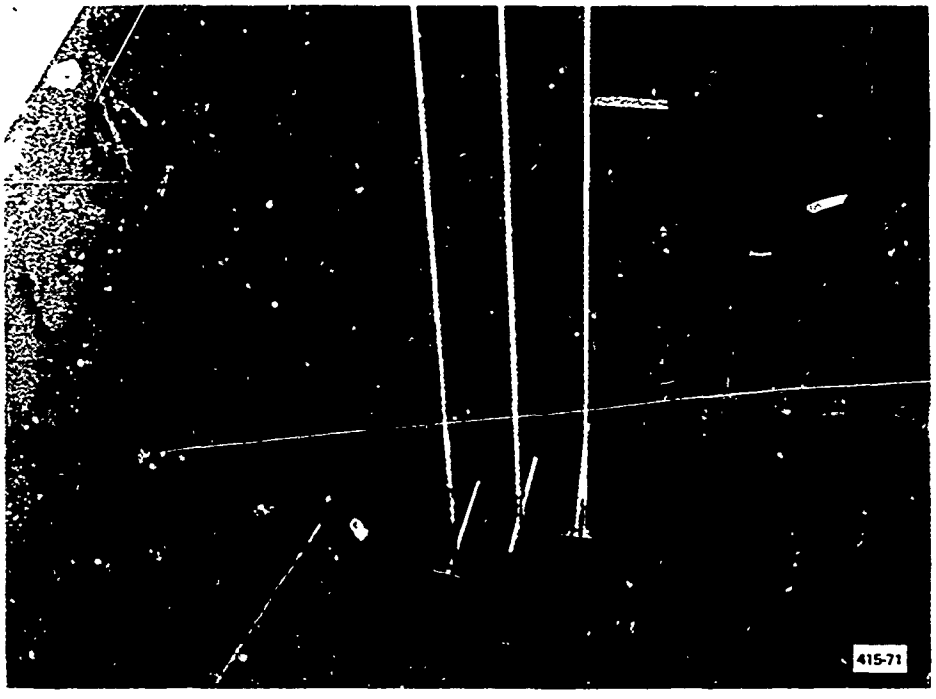

Figure 4-1 - Three-Target Placement

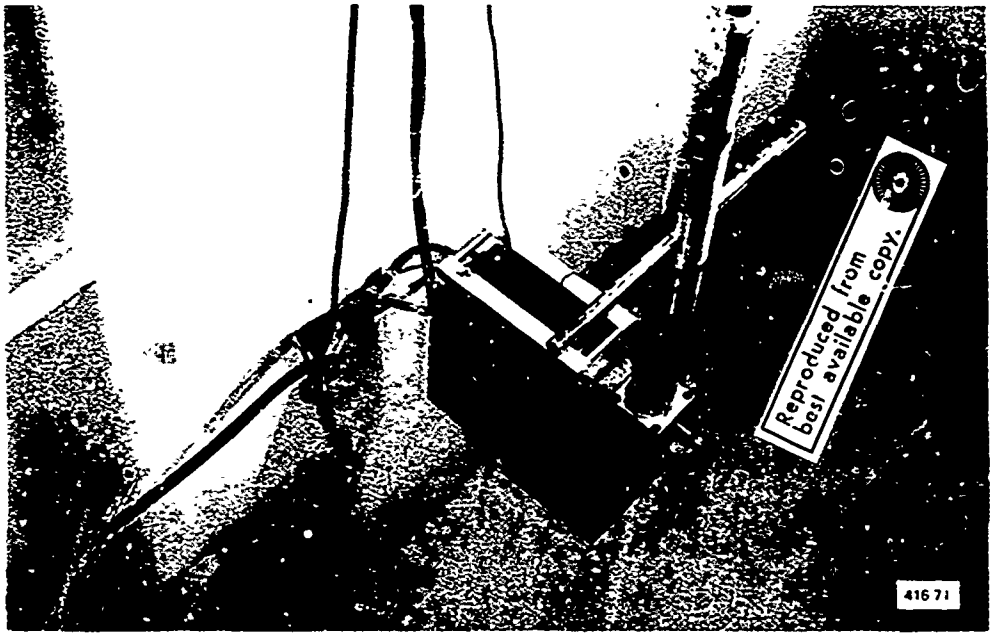

Figure 4-2 - Underwater Viewing System Receiver Array

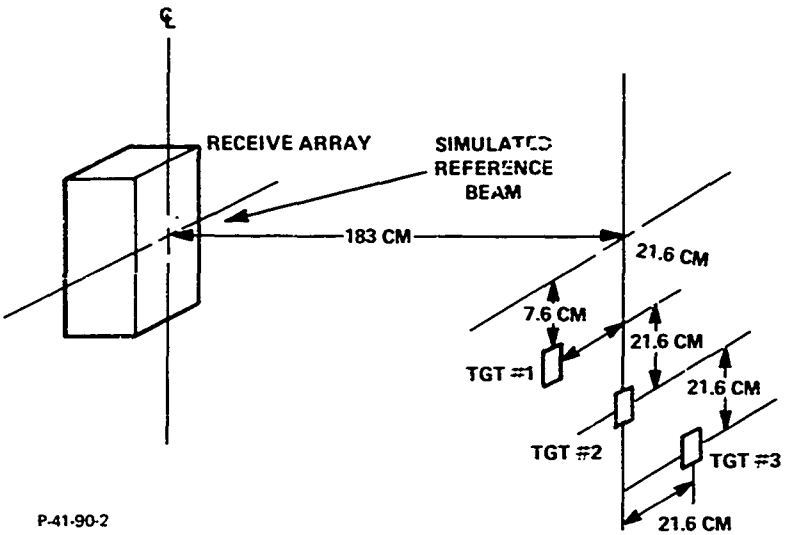

Figure 4-3 - Dimensional Layout of Targets and Receiver Array

the first lobe of the array. Since the angular position of the first lobe is equal to the system's viewing angle, the photograph provides a means for verifying this operational parameter.

Figure 4-8 schematically shows the half viewing angle and the angle for the centrum of the first lobe of the receive array. Referring to Figure 4-9, the measured horizontal distance between the image of two targets is 10 mm which corresponds to the actual target separation of 216 mm. The photograph reduction is then: $\frac{216}{10} \simeq 22$. The D.C. spot of the first-order diffraction appears 68 mm to the right of the zero-order D.C. spot. This corresponds to: 22 x 68 = 1,496 mm for the actual test setup. Since the image plane of the reconstruction corresponds to 1829 mm in the test setup, the angle of the first-order lobe can be calculated: $\theta = \text{Tan}^{-1} \frac{1496}{1829} \approx 39.3$ degrees. Design calculations show the first-order lobe to be at 42 degrees.

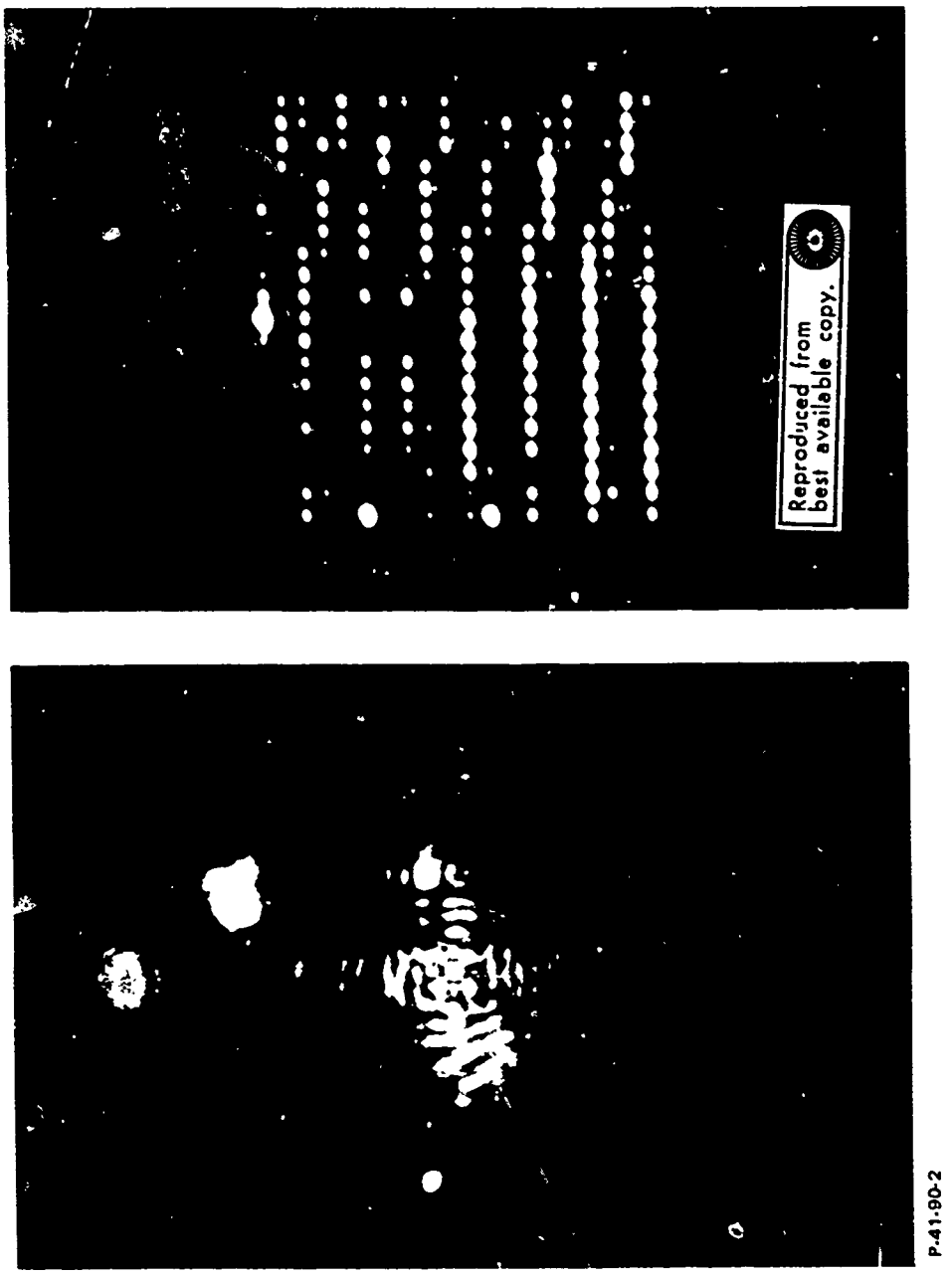

Figure 4-4 - Hologram and Reconstruction of Target No. 1

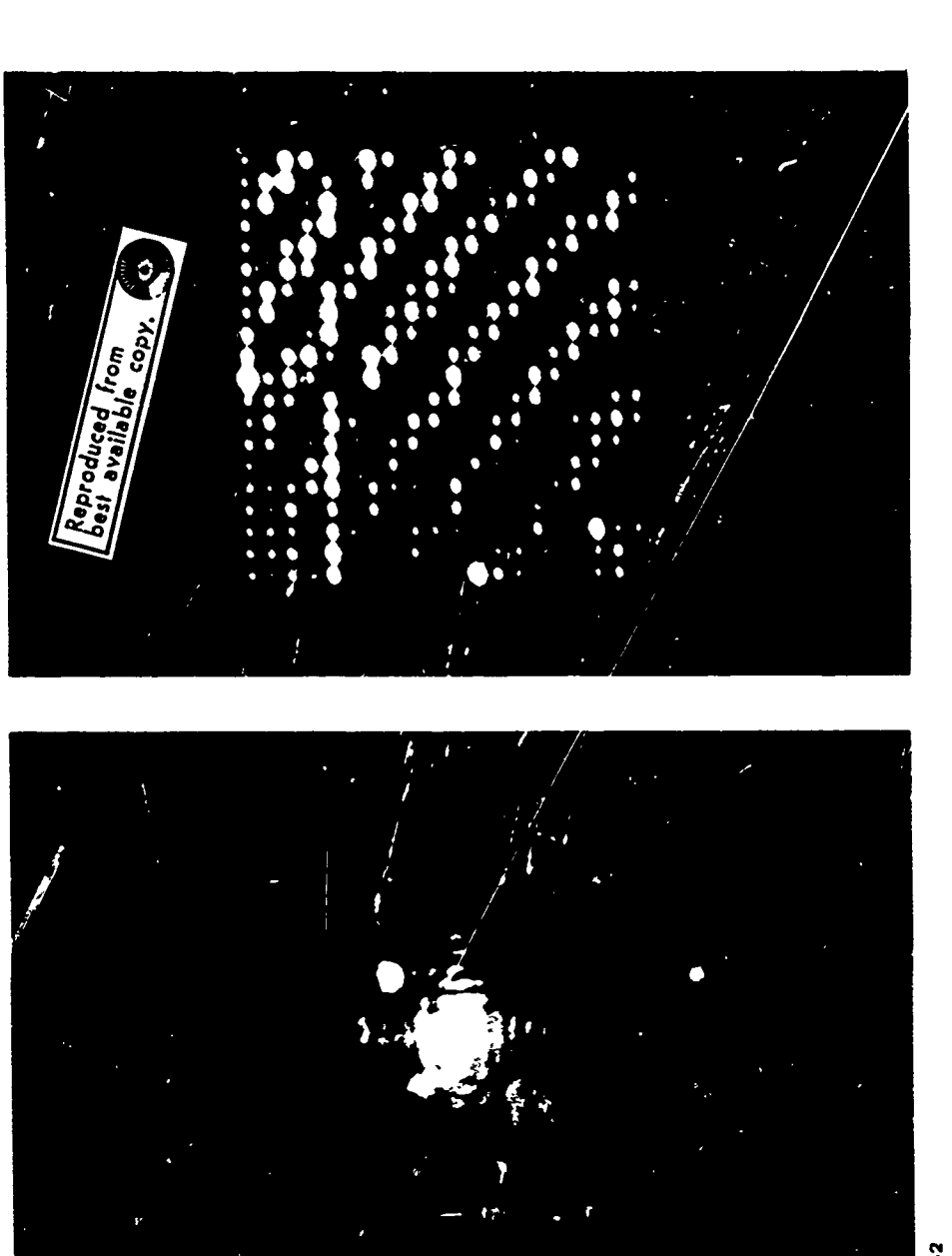

Figure 4-5 - Hologram and Reconstruction of Target No. 2

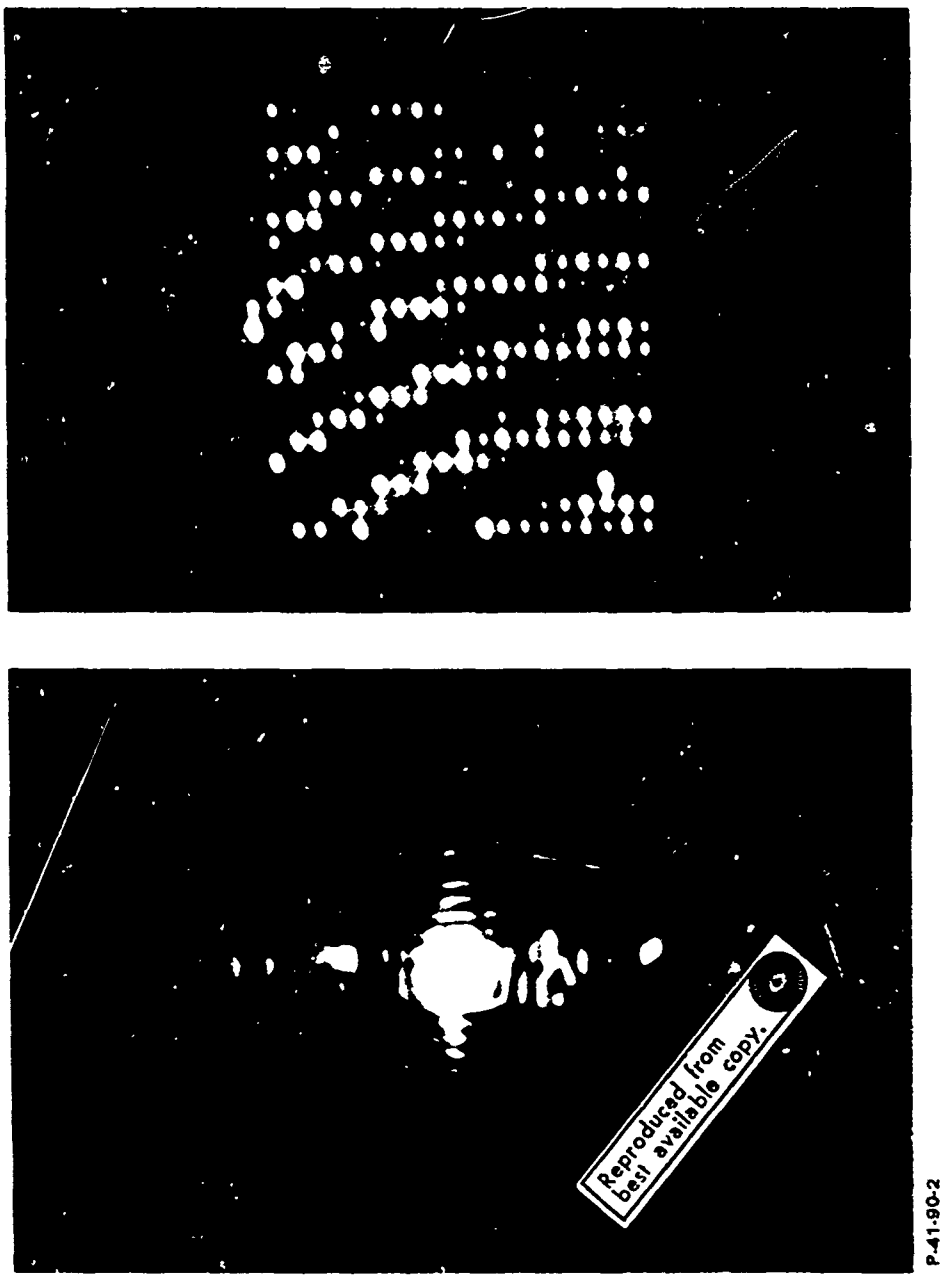

Figure 4-6 - Hologram and Reconstruction of Target No. 3

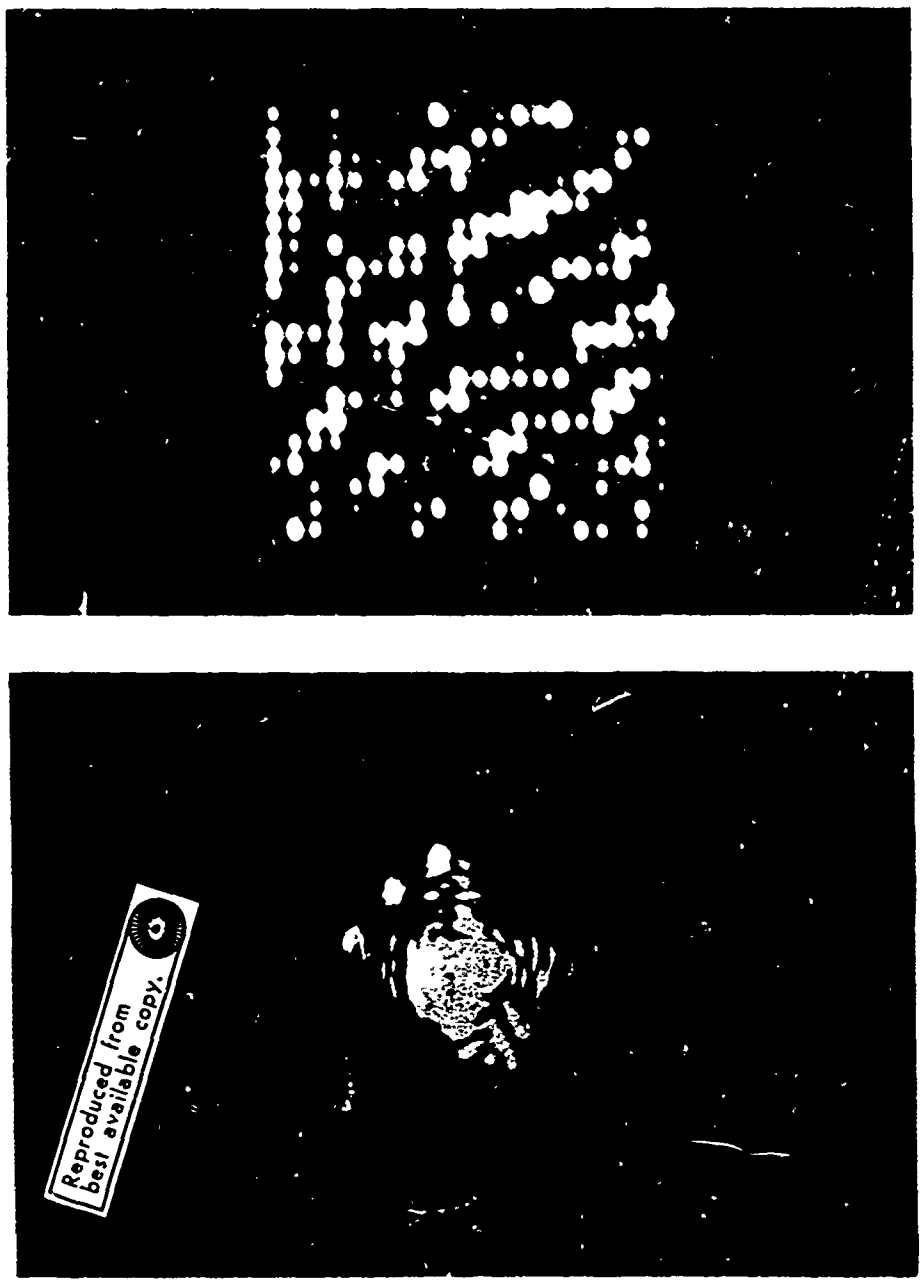

Figure 4-7 - Hologram and Reconstruction of Three Targets

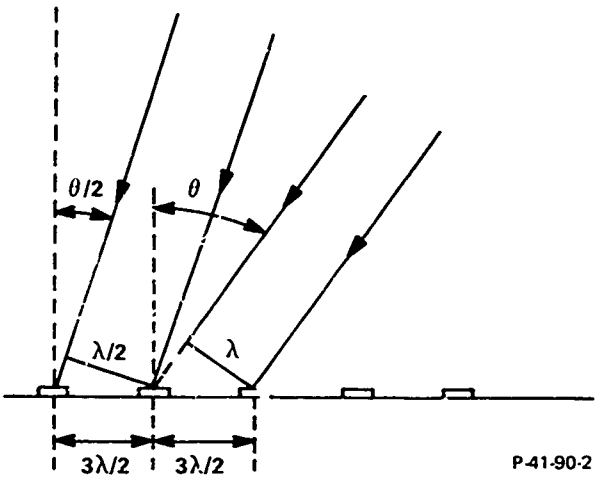

Figure 4-8 - Viewing Angle

The resolution expected for this experiment is very close to that observed experimentally. The aperture function (MTF) for a square array is, in one of the dimensions,

$$A \left| \frac{\sin (\pi a/\lambda \sin \phi}{(\pi a/\lambda) \sin \phi} \right|^2$$

where a is the array side (18 cm) and ϕ is the incident angle from the center. This function falls to 1/e when $(\pi a/\lambda) \sin \phi \approx \pi/2$. In the present experiment, $a/\lambda = 30$ and thus $\phi = \sin^{-1} (1/60)$ is the theoretical angular resolution. At an object distance of 1829 mm, this represents an apparent widening of the object by 30.5 mm each side. Thus, we expect the image of the disc to be approximately $\frac{137 \text{ mm}}{22} = 6.2$ mm on a side. In the reconstruction photograph, the reconstruction image measures between 6 mm and 7 mm.

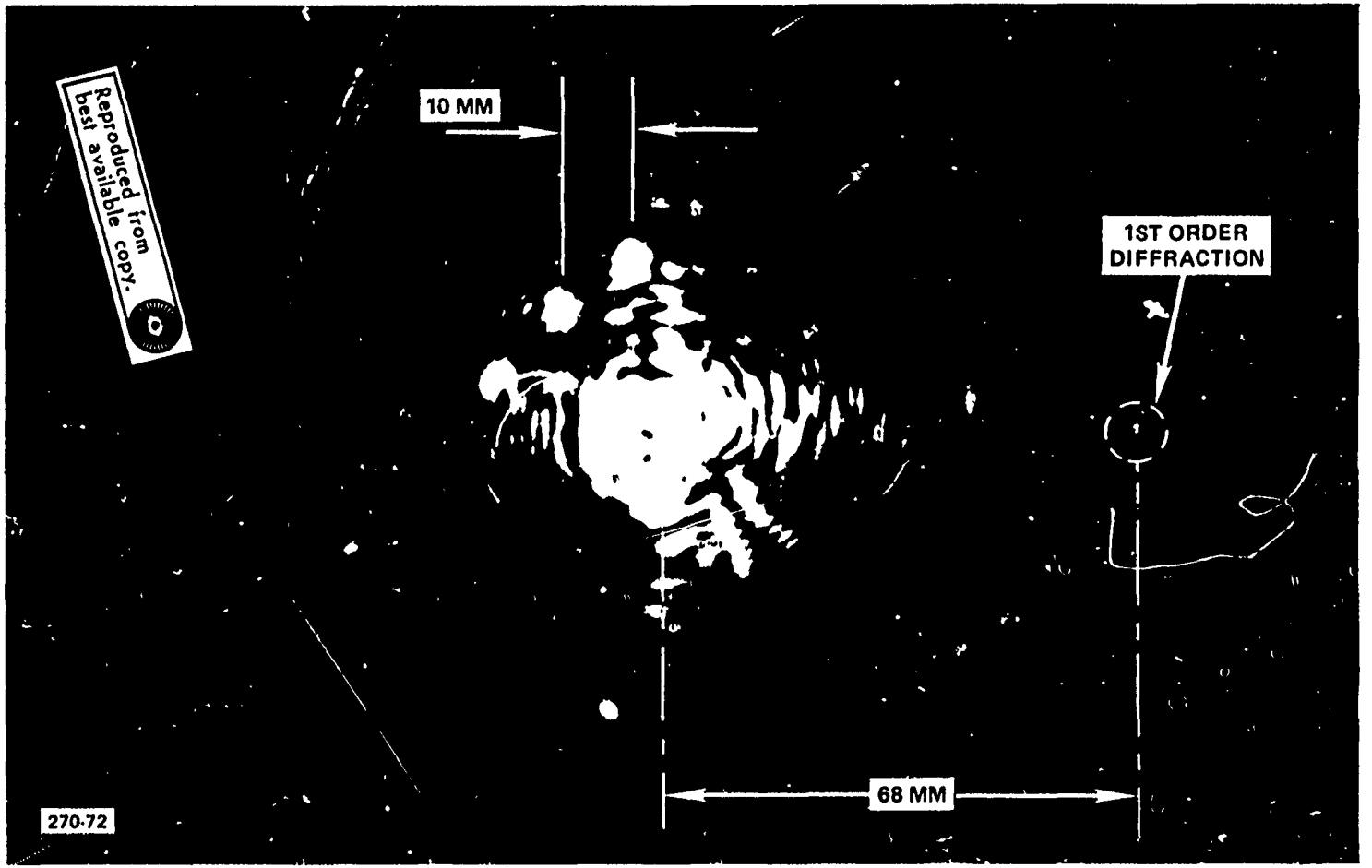

Figure 4-9 - Target Separation Measurements
(Taken on enlarged version of Figure 4-7)

4.1.2 Velocity Test

The second major experiment carried out with the underwater viewing system was performed to verify its capability to image moving targets. Two types of effects are noted. One type is essentially the familiar Doppler effect, while the other is essentially image blurring due to lateral object motion which occurs in amy form of imaging.

4.1.2.1 Primary Doppler Effects

If an object, located a radial distance $\underset{\sim}{r}$ from the array center, is moving at an arbitrary velocity $\underset{\sim}{v}$ as shown in Figure 4-10, the phase change rate at the center of the array is

$$\dot{\phi} = \frac{d\phi}{d\lambda} = 2 \times \frac{2\pi}{\lambda} \hat{\underset{\sim}{r}} \cdot \underset{\sim}{v}$$

where $\hat{\underset{\sim}{r}}$ is the unit vector along $\underset{\sim}{r}$ and $\underset{\sim}{v} = d\underset{\sim}{r}/dt$. We assume that the transmitter is also at the array center; the factor 2 arises because it is an active viewing system. In the Doppler viewpoint of this effect, it is just $-\Delta\omega$, where $\Delta\omega$ is the Doppler shift. The incoming signal at the ℓ^{th} element is

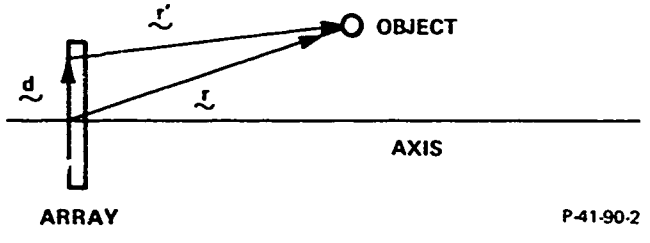

Figure 4-10 - Doppler Effect

$$A_\ell e^{i\phi_\ell} e^{i\dot{\phi}t} e^{-\omega t}$$

where ϕ_ℓ is the holographic phase information, ω is the transmitter frequency which is equal to the system reference frequency, and $-\dot{\phi}$ is the Doppler shift.

This signal, when mixed with the system reference signal at frequency ω, results in a product whose D.C. component (or, at least, low frequency component) is, for the ℓ^{th} element,

$$F_\ell(t) = A_\ell e^{i\phi_\ell} e^{i\dot{\phi}t}$$

In addition to this, there are also terms in the mixed signal at frequencies near 2ω, 4ω, etc., because the reference signal is a square wave. These are not of interest, however, because of the integration which follows. The mixer output is integrated for a period τ resulting in an output at the ℓ^{th} integrator

$$G_\ell(\tau,\phi) = A_\ell \, \mathrm{Re} \int_0^\tau e^{i\phi_\ell} e^{i\dot{\phi}t} \, d\tau$$

$$= \frac{A_\ell}{\dot{\phi}} \left[\cos\phi_\ell \sin\dot{\phi}\tau + \sin\phi_\ell (1-\cos\dot{\phi}\tau)\right]$$

$$= \frac{A_\ell}{\dot{\phi}/2} \sin\dot{\phi}\tau/2 \, \cos(\phi_\ell - \dot{\phi}\tau/2)$$

$$\text{i.e., } G_\ell(\tau) = \frac{A_\ell \lambda}{2\pi \hat{\underset{\sim}{r}} \cdot \underset{\sim}{v}} \sin\left(\frac{2\pi\tau}{\lambda} \hat{\underset{\sim}{r}} \cdot \underset{\sim}{v}\right) \cos\left(\phi_\ell - \frac{2\pi\tau}{\lambda} \hat{\underset{\sim}{r}} \cdot \underset{\sim}{v}\right)$$

As a function of $\hat{\underset{\sim}{r}} \cdot \underset{\sim}{v}$, $|G_\ell|^2$ falls off as a $|\text{sinc}|^2$ function with increasing $\hat{\underset{\sim}{r}} \cdot \underset{\sim}{v}$. As a function τ, the function $|G_\ell|^2$ is periodic, with zeros at integral values of $2\hat{\underset{\sim}{r}} \cdot \underset{\sim}{v} \frac{\tau}{\lambda}$. There is neither an overall increase or decrease with increasing time. We note, however, that any unshifted returns which are coherent with the reference and any incoherent noise both increase with τ(as τ and τ 1/2, respectively), and thus the signal-to-noise decreases with increasing τ. If noise and unshifted interference are negligible, though, the result is merely periodic in τ.

Figure 4-11 schematically depicts three signals of different frequencies and the corresponding integrator outputs as a function of τ. Square waves are used for this illustration so that the resulting integrator output variations are independent of amplitude. Waveform (A) of Figure 4-11 is the reference signal which has a fundamental frequency of $\frac{1}{8X}$ and waveform B-1 represents an off-frequency signal which, when mixed with the reference signal and integrated, results in waveform B-2. The fundamental frequency of waveform B-1 is $\frac{1}{10X}$, while the beat frequency resulting from mixing and integration is $f_1 - f_2 = \frac{1}{8X} = \frac{1}{10X} = \frac{1}{40X}$.

Waveform C-1 is slightly lower in frequency than B-1 and, when mixed with the reference signal and integrated, results in output C-2. It can be seen that as the signal frequency moves away from the reference frequency, the resultant output is reduced in amplitude as well as in period. As previously noted, zeros in the output occur at half-integral values of the difference frequency produced by the mixing action. Since the interchanging of waveform A with B-1 or C-1 has no

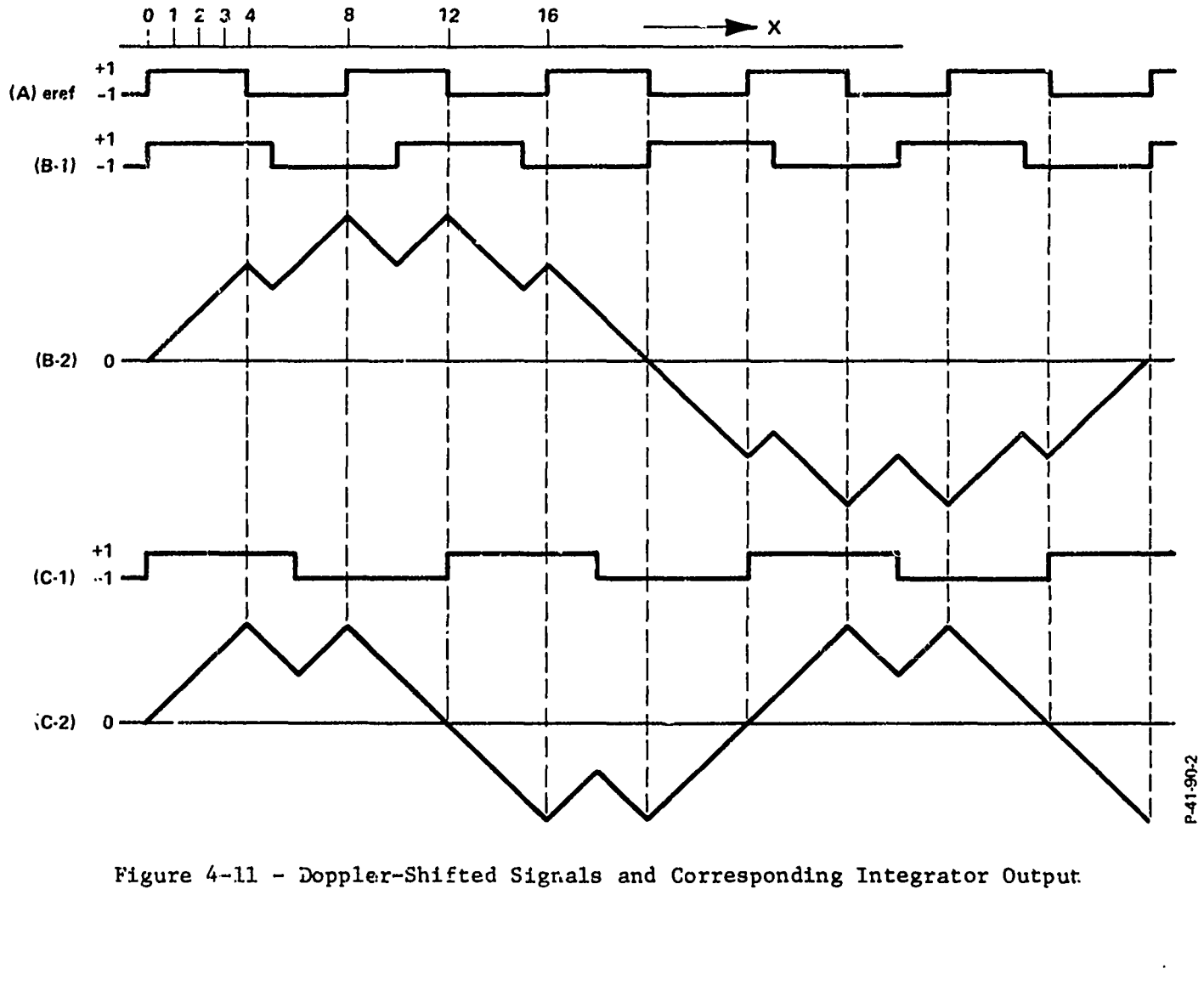

Figure 4-11 - Doppler-Shifted Signals and Corresponding Integrator Output

effect on the integrator output, a signal shifted to a higher frequency has the same affect as a signal shifted to a lower frequency, as would be the case in up-and-down Doppler.

Referring to Equation (1), the cosine term contains a Doppler component as well as a term containing the desired holographic information (i.e., A_ℓ and ϕ_ℓ). Since the Doppler component is (except for the effects discussed in the subsection below on lateral motion) common to all elements within the array, it merely represents on overall shift in the apparent phase of all the singles as seen at the integrator outputs and does not modify the holographic content in any non-trival sense.

The first null in G_ℓ (Equation 1) occurs at

$$\hat{\underset{\sim}{r}} \cdot \underset{\sim}{v}\tau/\lambda = 1/2.$$

When the velocity vector is in the most undesirable direction,

$$\hat{\underset{\sim}{r}} \cdot \underset{\sim}{v} = v$$

and Equation (2) is satisfied with

$$v_c = \lambda/2\tau$$

for fixed τ, or

$$\tau_c = \lambda/2v$$

for fixed N.

Figure 4-12 shows a sketch of the target mechanism used for the velocity measurement. The arm of the test fixture rotates at an angular velocity determined by a variable D.C. motor. The receive array is aligned to one side of the test fixture so that it only receives returns from a target passing through its field of view and does not receive returns from the test fixture supporting structure. Figure 4-13 shows the installed velocity test fixture.

Due to cost considerations, the test fixture was designed for a maximum target velocity of 8 knots rather than the proposed 10 knots. This reduction in target velocity can be compensated for by increasing the receive time (τ in Equation 1) until nulls occur in the integrator outputs.

The target velocity was set at approximately 7.6 knots which (using Equation 3) results in the first null appearing at τ = 765 μsec. Other nulls will occur at τ = 1530 μsec, 2295 μsec, etc.

The holograms were made by first setting the receive time as short as possible (approximately 30 μsec) and adjusting the system delay (range) so that the hologram would just appear on the monitor. This initial adjustment ensured that a target return would be present during the entire integration period so that the effective integration time is always equal to the nominal recieve time. The possibility of having a return only during the latter part of the integration period, as would be the case if the range delay was less than that required, is thereby avoided.

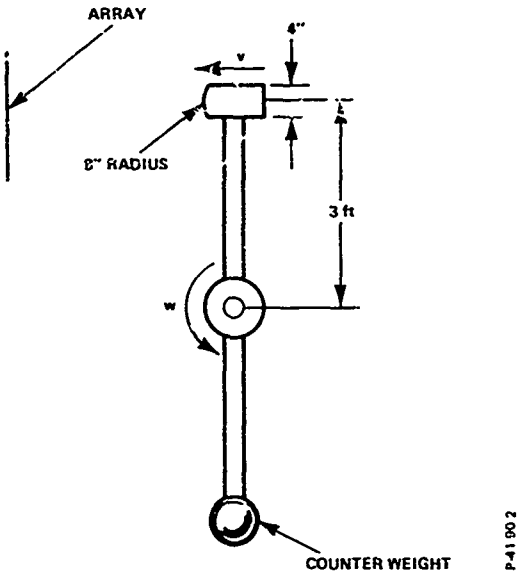

Figure 4-12 - Velocity Measurement Mechanism

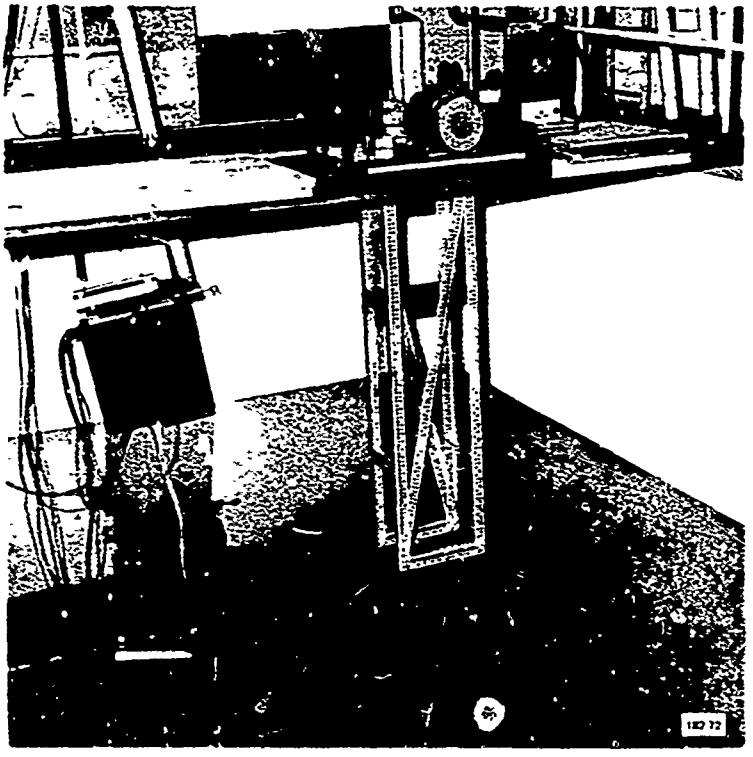

Figure 4-13 - Velocity Test Fixture Installation

Figures 4-14A through 4-14K show the holograms and reconstructed images of the moving target with receive times ranging from 200 μsec to 1200 μsec in 100 μsec steps. A degradation of the hologram and the reconstructed image is noted between 600 μsec and 800 μsec as the integrator outputs pass through the first null. At 1100 μsec, the hologram is again starting to wash out as the outputs approach the second null. It is also important to note that the background noise is becoming fairly significant as the integration time is increased to its maximum of 1200 μsec. Even at 1000 μsec and 7.6 knots (essentially equivalent to 250 μsec and 30 knots), good holograms are obtained, as Figure 4-13I shows.

4.1.2.2 Blurring due to Lateral Motion

It is clear from the foregoing consideration that the effect of object velocity on the system is essentially similar to the Doppler effect. Historically, there has been a distinction made between the cases (a) where the Doppler shift is significant ($\hat{r} \cdot v \neq 0$) and (b) where the object moves laterally with respect to the array (e.g., crosses the axis normally) and where $\hat{r}$ and v defined in the figure are orthogonal ($\hat{r} \cdot v = 0$). It is worth pointing out, however, that both of these effects can readily be described as due to the Doppler effect.

$$-\frac{1}{2\pi}\dot{\phi} = \Delta f = -\frac{2\hat{r} \cdot v}{c} f = \frac{2\hat{r} \cdot v}{\lambda}$$

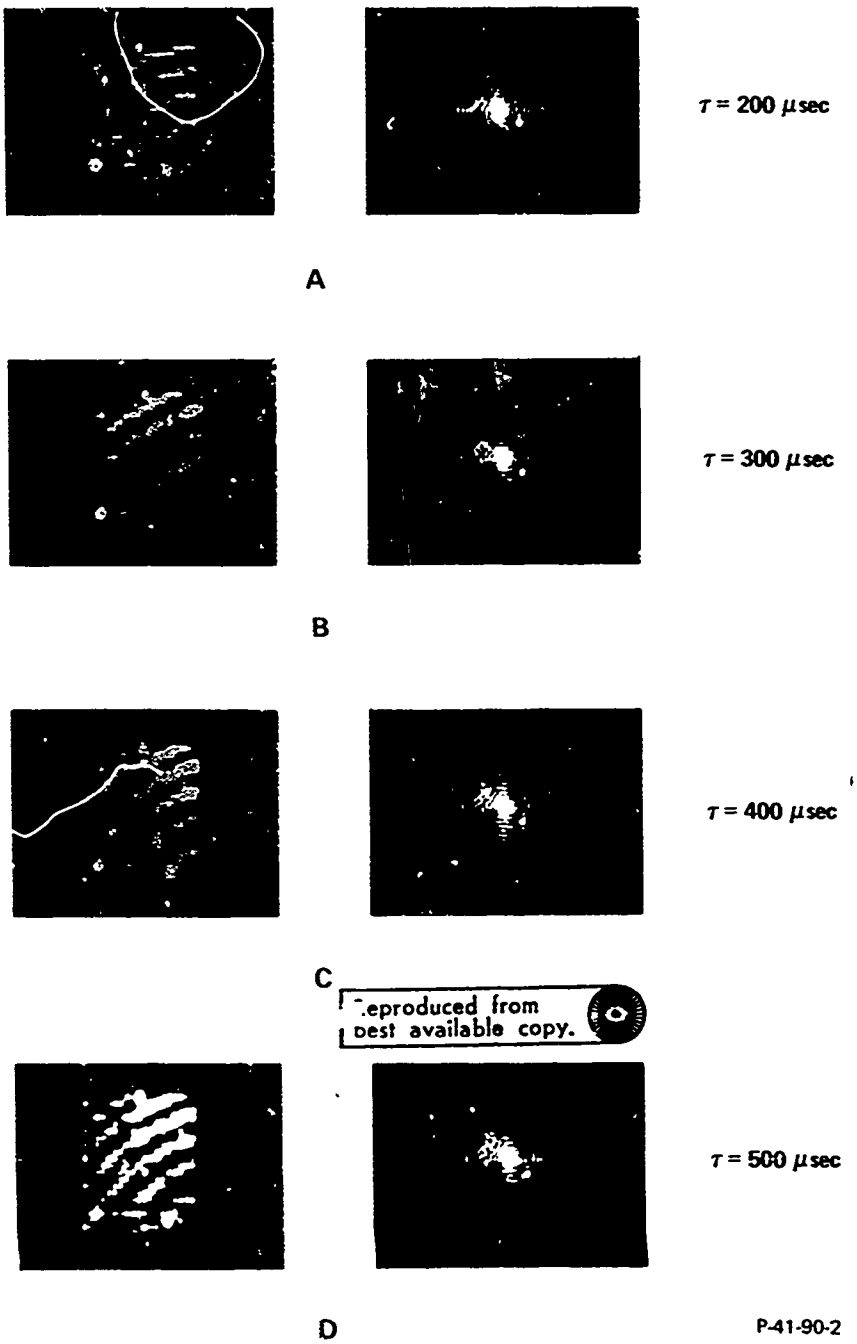

Figure 4-14 - Doppler Effects on Reconstructed Image (1 of 3)

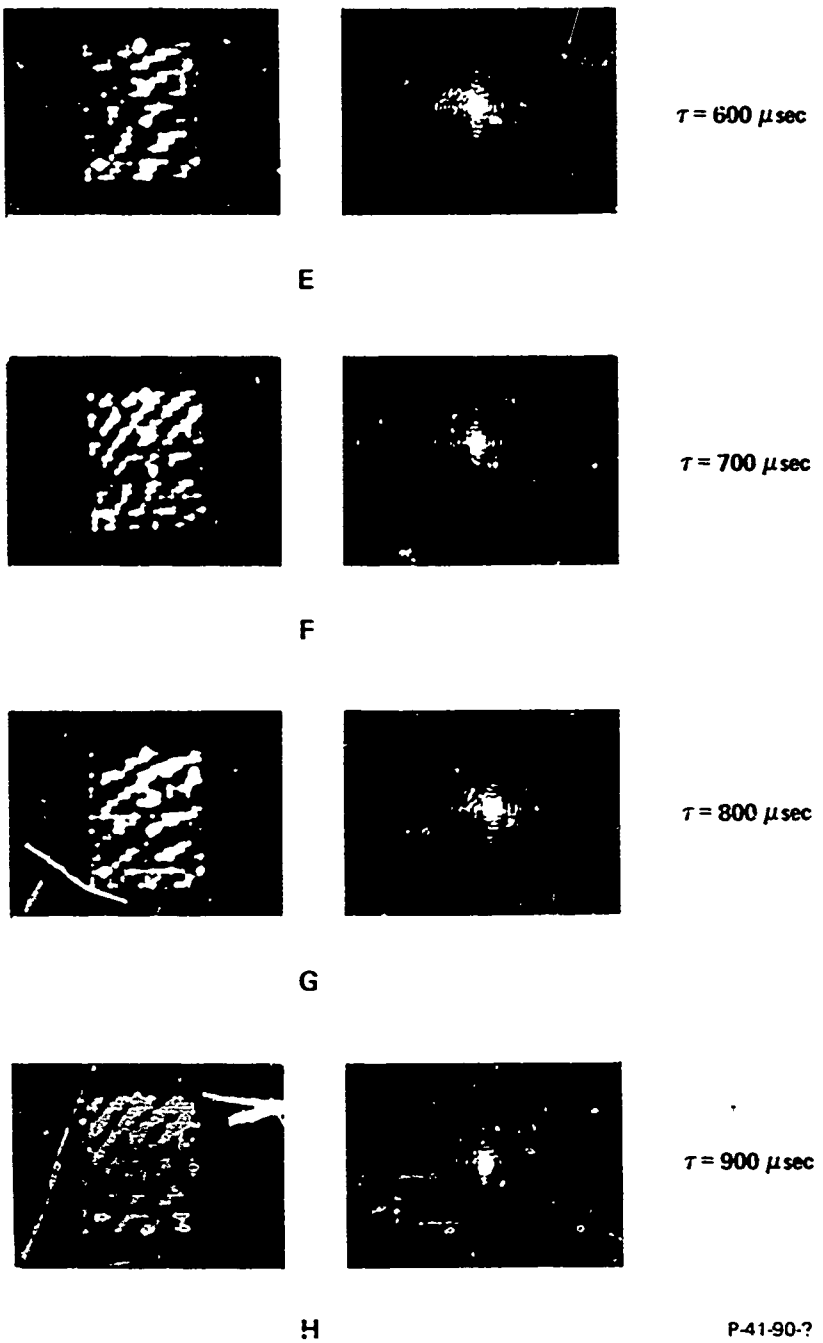

Figure 4-14 - Doppler Effects on Reconstructed Image (2 of 3)

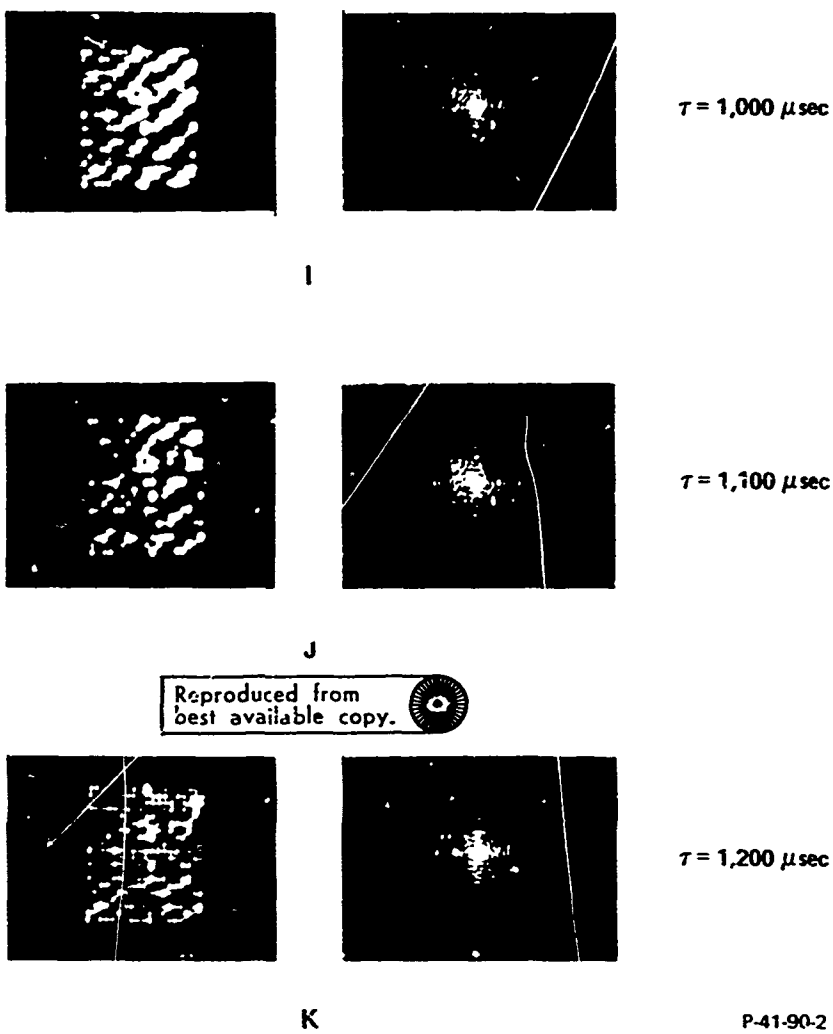

Figure 4-14 - Doppler Effects on Reconstructed Image (3 of 3)

As noted, we are interested in the effects which occur when $\hat{\underset{\sim}{r}} \cdot \underset{\sim}{v}$ is zero for non-zero $\underset{\sim}{v}$. Although the Doppler shift at the center of the array is zero, because of the finite extent of the array (necessary to obtain acceptable resolution), there is a Doppler shift in other regions of the array.

At a distance $\underset{\sim}{d}$ from the center of the array, the Doppler shift is (see Figure 4-10)

$$\Delta f = -\frac{2\hat{\underset{\sim}{r}}' \cdot \underset{\sim}{v}}{c} f = \frac{2\underset{\sim}{d} \cdot \underset{\sim}{v}}{\lambda|\underset{\sim}{r}'|}$$

since $\underset{\sim}{r} \cdot \underset{\sim}{d} = 0$. Hence

$$|\Delta\phi| = \frac{4\pi\tau}{\lambda|\underset{\sim}{r}'|} \; |\underset{\sim}{d} \cdot \underset{\sim}{v}| < \pi/2$$

Thus, the velocity effects are small only over a region of the array such that $\underset{\sim}{d}$ satisfies

$$\frac{|\underset{\sim}{d} \cdot \underset{\sim}{v}|}{|r'|} < \frac{\lambda}{8\tau}$$

Therefore, the effective aperture of the viewing system is reduced from a square of side L to an L x L' rectangle, where

$$L' \frac{2\lambda}{8\tau\dot{\phi}} < L$$

when the projection of $\underset{\sim}{v}$ on the array plane is parallel to one of the array sides ($\dot{\phi}$ is the angular velocity $|\underset{\sim}{v}|/|r'|$). Thus, the reduced effective aperture results in a loss of resolution parallel to the motion of the object, which is equivalent to blurring.

We note that this effect is range-dependent in the sense that an object moving at constant velocity produces a smaller effect at the longer ranges

The reduced resolution in terms of d' is

$$\Delta\theta \sim \frac{\lambda}{\pi d'}$$

i.e.,

$$\Delta\theta \approx \frac{4\dot{\phi}\tau}{\pi}$$

which is as close to the expected value ($\Delta\theta' = \dot{\theta}\tau$) for the blurring as one expects for such estimates. This effect is small. For $L/\lambda = 30$, $R = 150$ cm and $\tau = 150$ μsec, V must be in the order of 150 knots to be significant.

Since maximum velocity obtainable with the test fixture does not significantly approach the required velocity of 150 knots, an experimental verification of the above was not initiated, especially since the effect is so well-known.

SECTION 5

ANALYSIS OF SYNTHETIC APERTURES AND NON-PLANAR ARRAYS

Synthetic apertures were analyzed to determine possible trade-offs between hardware and software to realize an effective, large-area array. Non-planar arrays were analyzed to determine the requirements for arrays that would conform to the shape of a vessel's hull and thereby be more compatible with the requirements of naval architecture.

5.1 SYNTHETIC APERTURE ANALYSIS

The results of an analysis relating to a synthesis of large-area arrays using a small receive array and an array of transmitting elements were reported in the Interim Report dated January 1971.[3] The objective of this analysis was to determine whether a system comrised of a receiving array of n by $\bar{n}$ elements and a transmitting array of m by $\bar{m}$ elements provide the same effective aperture as a system comprised of a receive array of nm by $\bar{n}\bar{m}$ elements and a single transmitter, thereby considerably reducing the amount of hardware in the system. The configuration for this analysis is illustrated in Figure 5-1.

The analysis showed that, corresponding to a given activated element $(m, \bar{m})$ in the transmit array, a correction which is range dependent and linear in $(n, \bar{n})$ of the receive array must be added to the phase. This correction could be introduced during the recording of the hologram or during the reconstruction process.

If we choose to correct for this effect in the recording process, the electronic programming for the reference beam should allow a choice

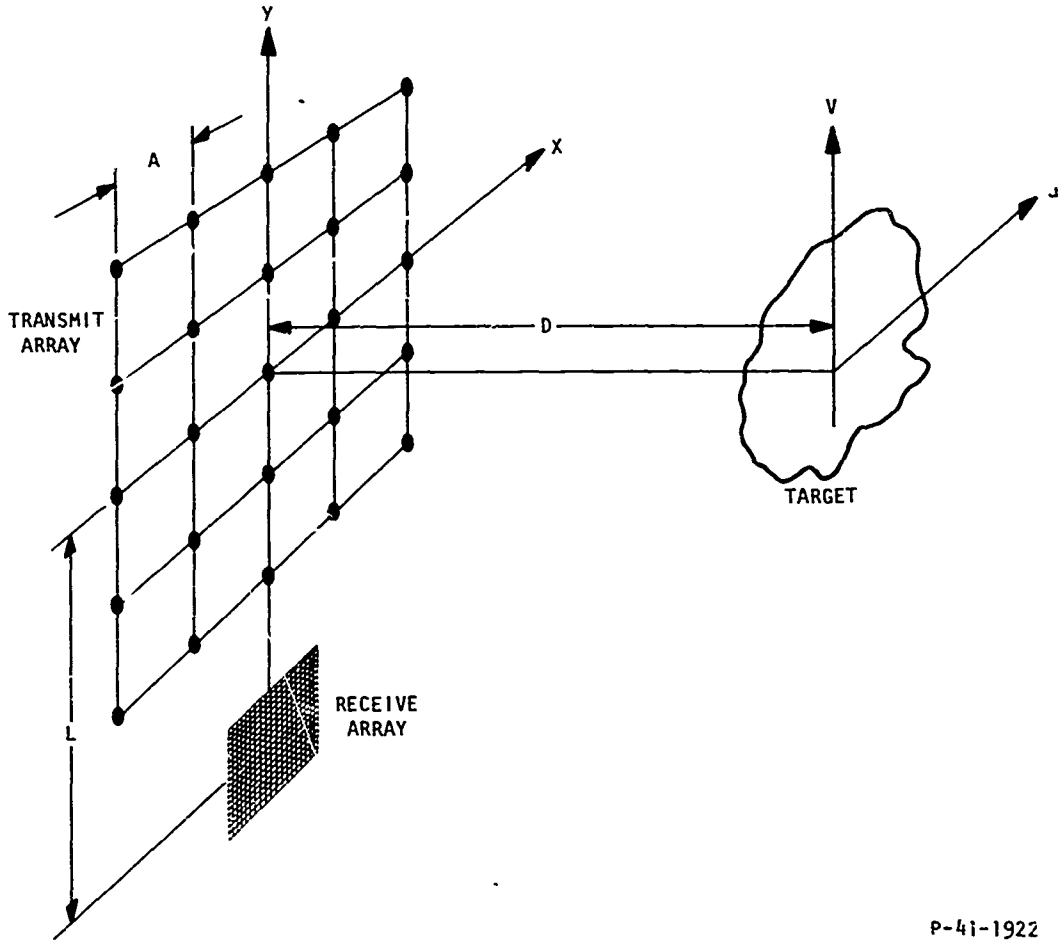

Figure 5-1 - Source and Receive Arrays Configuration

of various phase rates along the scanned coordinate. We do not anticipate the need to quantize the phase any more than 45 degrees ($\pi/4$). On the other hand, if we computerize the electronic reconstruction system, the linear non-uniform phase correction can be introduced externally. An analog correction for these phase changes is also possible, i.e., by having a correction filter, composed of linear fringes of proper spacing and orientation or a m x m set of prisms, in contact and in registration with the hologram.

The system in operation would require the activation of the source transducers (transmitters) in sequence. A full holographic recording is performed after each source activation. Thus, by the time that all elements are activated, all ($\bar{n}\bar{n}\bar{m}\bar{m}$) sampled points in the aperture plane have been detected and displayed. However, operating the source transducers in sequence results in a disadvantage in that only essentially static holograms can be obtained, and moving targets cannot be detected and imaged.

5.2 NON-PLANAR ARRAY ANALYSIS

In much of holographic theory, the hologram detector, or detectors, are assumed to lie on a plane surface. However, one of the advantages of holography for underwater viewing is the possibility that the detector array can instead conform to the shape of a vessel's hull and thereby be more compatible with the requirements of naval architecture. In the present analysis, we examine (a) the effect on the hologram of an arbitrarily-shaped (non-pathological) surface, and (b) methods of handling the difference between this shape and a plane.

5.2.1 Arbitrary Hologram "Surface"

We shall carry out our analysis for one-dimensional holograms since this reduces the notational complexity and retains the important aspects of the problem. The extension to two-dimensional holograms is straightforward.

As shown in Figure 5-2, the "surface" (a line in our one-dimensional theory) is described by the function $y(x)$, where x is the lateral coordinate and y is the longitudinal coordinate. For convenience,

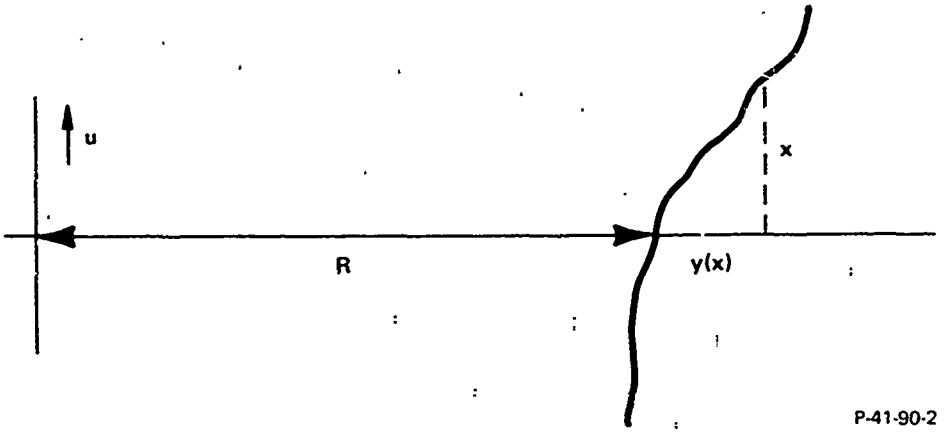

Figure 5-2 - Arbitrary Surface

we shall, without loss of generality, take the (one-dimensional) object as a normally-illuminated transparency g(u). The usual planar hologram 'surface' corresponds to y = o, of course.

The distance from a point u on the object to a point at x on the surface is

$$\ell(x, u) = \left\{ [R + y(x)]^2 + (x - u)^2 \right\}^{1/2} . \qquad (1)$$

In the Fresnel approximation, we expand this as

$$R + \frac{(x - u)^2}{2R} + y(x) \qquad (2)$$

The first term is a constant; the second term in $(x - u)^2$ is the term which arises with the usual planar hologram. The term y(x) is the new term due to the array shape.

Before treating the general problem, it is instructive to examine the low orders of a Taylor series expansion of y(x):

$$y(x) = xy'(o) + \frac{1}{2} x^2 y''(o) + \frac{1}{6} x^3 y'''(o) + \ldots \qquad (3)$$

The linear term in equation (3) gives rise to a linear term in x in equation (2). The linear term in equation (2), as we now show, merely gives rise to a lateral shift in the image upon reconstruction.

The hologram is, if we ignore the constant term in equation (2) and use the Fresnel approximation,

$$G(x) = \frac{1}{R} \int g(u)\, e^{\frac{ik}{2R}(x-u)^2}\, e^{iky(x)} \tag{4}$$

The surface shape affects the signal amplitude as well as its phase, because of the angle that the surface 'shows' to the object. However, this does not arise in the Fresnel approximation. The phase changes are quite definitely the most important. Moreover, the amplitude compensation is obvious and relatively easy to apply.

The linear contribution to equation (2) gives

$$G(x) = \frac{1}{R} \int g(u)\, e^{-\frac{ik}{2R}(x-u)^2}\, e^{ikxy'} \tag{5}$$

and the reconstructed image at a distance R is

$$\hat{g}(\xi) = \frac{k}{2\pi} \int G(x)\, e^{-\frac{ik}{2R}(x-\xi)^2}\, dx \tag{6}$$

$$= \frac{ke}{2\pi R}^{-\frac{ik}{2R}\xi^2} \int du\, g(u) \int e^{\frac{ikx}{R}(\xi-u+Ry')}\, e^{\frac{ik}{2R}u^2}\, dx \tag{7}$$

$$= e^{-\frac{ik}{2R}\xi^2} \int du\, g(u)\, e^{\frac{ikx}{2R}u^2}\, \delta(\xi - u + Ry') \tag{8}$$

$$= g(\xi + Ry')\, e^{iky'(\xi+Ry^{1/2})} \tag{9}$$

i.e.,

$$|\hat{g}(\xi)|^2 = |g(\xi + Ry')|^2 \tag{10}$$

Thus the image is shifted in position by Ry'(o) and given a phase shift. These are trivial effects.

The quadratic term in equation (3) also gives a quadratic phase term in equation(2). The effect of this is also relatively trivial - the image plane is shifted longitudinally by a small amount. The effect of such a quadratic phase term is seen by the following. We now have

$$G(x) = \frac{1}{R} \int du\, g(u)\, e^{\frac{ik}{2R}(x-u)^2}\, e^{\frac{ikx^2}{2}y''} \tag{11}$$

where we here ignore the linear term discussed above.* We now reconstruct at R' where $1/R' = 1/R + y''$:

$$\hat{g}(\xi) = \frac{k}{2\pi} \int G(x)\, e^{-\frac{ik}{2R'}(x-\xi)^2} \tag{12}$$

$$= e^{-\frac{ik}{2R'}\xi^2} \int du\, g(u)\, e^{\frac{ik}{2R}u^2}\, \delta\left(u - \frac{R}{R'}\xi\right) \tag{13}$$

$$= g\left(\frac{R}{R'}\xi\right) e^{\frac{ik}{2R'}\xi^2} \left(1 - \frac{R}{R'}\right) \tag{14}$$

i.e.,

$$|\hat{g}(\xi)|^2 = \left|g\left(\frac{R}{R'}\xi\right)\right|^2 \tag{15}$$

The factor R/R' in the argument merely represents the change in magnification due to the surface curvature.

Thus, if a surface has no derivatives of third order or higher, then no special steps are necessary to compensate for the surface, apart from aberrations.

*This is done only to avoid carrying along the additional notational complexity and the lateral image shift discussed above. It is not generally valid from a computational point of view.

We now return to the arbitrary 'surface'. We intend to show that compensation can always be provided during the reconstruction process. We use the general form $\ell(x, u)$ for the distance from object point to hologram point and, in accordance with the usual integral form, write the holographic transform as

$$G(x) = \int du\ g(u)\ e^{ik\ (x,u)}\ \frac{\cos\ \theta\ (x,\ u)}{\ell(x,\ u)} \tag{16}$$

where $\cos\ \theta\ (x, u) = R + y(x)/\ell(x, u)$. Thus,

$$G(x) \simeq \frac{e^{ikR}}{R} \left[\int_{du}\ g(u)\ e^{\frac{ik}{2R}\ (u-x)^2} \right] e^{iky(x)} \tag{17}$$

in the approximation made in equation (2). The surface shape compensation is accomplished by using $\ell\ (x, \xi)$ upon reconstruction:

$$\hat{g}(\xi) \simeq \frac{k}{2\pi} \int dx\ G(x)\ e^{-ik\ell\ (x,\xi)} \tag{18}$$

$$\simeq \frac{k}{2\pi R} \int du\ g(u) \int dx\ e^{\frac{ik}{2R}\left[(x-u)^2\ -\ (x-\xi)^2\right]} \tag{19}$$

$$= g(\xi) \tag{20}$$

Thus, in the Fresnel approximation, the phase errors of an arbitrarily-shaped array surface may be exactly compensated in the reconstruction. We note that it may also be exactly compensated during recording of the hologram since, in the Fresnel approximation, the phase term depends only on the array coordinates (x) and not on the object coordinates (u). In other words, if

$$\tilde{G}(x) + G(x)\ e^{-iky(x)} \tag{21}$$

is recorded instead of $G(x)$, then no phase correction is necessary during reconstruction.

However, when the Fresnel approximation made in obtaining equation (2) is not valid, the situation is not so clear. First, it is not obvious that any substantially complete compensation is possible, even during reconstruction. However, general considerations, including the analysis given below, suggest that this is possible. Secondly, it is doubtful whether any reasonably implementable corrections are possible prior to the recording of the hologram.

The Fresnel approximation breaks down if $ka^4/8R^3$ is no longer small compared with unity, where a is the maximum value of $|x - u|$. In the system designed and built for ONR by Bendix, the Fresnel approximation is pretty good for R greater than 3 feet. Alternatively, the approximation of equation (2) also becomes invalid if the quantity $ka^2y/2R^2$ is not small. For values of y as high as 10λ, this approximation is also adequate for R greater than 3 feet. The system is not designed or intended for distances much less than about 5 feet and the approximation made in equation (2) is thus a good one. However, larger arrays are likely to be employed in the future, and both a and y would then be larger than assumed above. Thus, the near-field case is still of appreciable interest.

The surface shape compensation is accomplished by using $\ell(x, \xi)$ upon reconstruction:

$$\hat{g}(\xi) = \frac{k}{2\pi} \int dx\, G(x)\, e^{-ik\ell(x,\xi)} \cos\theta(x, \xi) \tag{22}$$

where

$$G(x) = \int du\, g(u)\, \frac{e^{ik\ell(x,u)}}{\ell(x, u)} \cos\theta(x, u) \tag{23}$$

Hence

$$\hat{g}(\xi) = \frac{k}{2\pi} \int du\, g(u) \int dx\, e^{ik\ell\,(x,u)-\ell(x,\xi)}\, \frac{\cos\theta\,(x,\,u)\,\cos\theta\,(x,\,\xi)}{\ell(x,\,u)} \tag{24}$$

The integral over dx cannot be handled exactly in this general form. However, we have a general approximation method - the method of stationary phase - which we can use to obtain some useful general results.

We consider the integral

$$I = \int dx\, e^{i\phi(x)} \tag{25}$$

If there are changes in ϕ appreciably larger than a wavelength, the main contribution to the integral arises from regions around points of stationary phase, i.e., where $d/dx\ \phi(x) = o$. Then

$$I \approx \sum_{\ell} e^{i\phi_\ell} \int dx\, e^{\frac{i}{2}\frac{d^2}{dx_\ell^2}\ \phi(x_\ell)\ (x-x_\ell)^2} \tag{26}$$

where the different ℓ values range over the different points x_ℓ at which the phase is stationary. If we apply this method to equation (18), we are looking for regions where

$$\frac{d}{dx}\,\ell\,(x,\,u) = \frac{d}{dx}\,\ell\,(x,\,\xi) \tag{27}$$

The most obvious solution to this equation is when $u = \xi$, when it is satisfied for all x. Because it is satisfied for all x, it is also the dominant contribution to equation (18). However, other solutions of equation (26) do arise in general. They may, perhaps, be termed 'accidental' solutions since they will occur only for certain specific

values of x, u, ξ, and will therefore give only small contributions to equation (18).

We therefore take

$$\ell(x, u) - \ell(x, \xi) \approx (u - \xi) \frac{d}{d\xi} \ell(x, \xi) \tag{28}$$

and thus

$$\hat{g}(\xi) \approx \frac{k}{2\pi} \int du\, g(u) \int dx\, e^{ik\ell'(x,\xi)(u-\xi)} \frac{\cos^2 \theta (x, \xi)}{\ell(x, \xi)} \tag{29}$$

$$= \frac{k}{2\pi} \int dx\, \Gamma[\hat{x}'(x, \xi)]\, e^{-ik\xi\ell'(x,\xi)} \frac{\cos^2 \theta (x, \xi)}{\ell(x, \xi)} \tag{30}$$

where $\ell' = \gamma\ell/\gamma\xi$ and

$$\Gamma(\lambda) = \int du\, g(u)\, e^{-iku\lambda} \tag{31}$$

is the Fourier transform of g(u).

We now write $f = \partial\ell(x,\xi)/\partial\xi$ so that we obtain

$$\hat{g}(\xi) \approx \frac{k}{2\pi} df \left(\frac{dx}{df}\right) e^{-ikf\xi}\, \Gamma(f)\, \frac{\cos^2 \theta}{\ell} \tag{32}$$

Now

$$f = \frac{\gamma}{\gamma\xi} \left[\left(R + y(x)\right)^2 + (\xi - x)^2\right]^{1/2} = \frac{\xi - x}{\ell} \tag{33}$$

and thus

$$\frac{df}{dx} = -\frac{1}{\ell^2} \left[\ell + (\xi - x) \frac{\gamma\ell}{\gamma x}\right] = -\frac{1}{\ell^3} \left[\ell^2 - (\xi - x)^2\right] \tag{34}$$

$$= -\frac{(R + y)^2}{\ell^3} \tag{35}$$

But

$$\cos \theta = \frac{R + y}{\ell} \quad \text{so that} \tag{36}$$

$$\hat{g}(\xi) \approx -\frac{k}{2\pi} \int df\, e^{-ikf\xi}\, \Gamma(f) = \bar{g}(\xi) \tag{37}$$

where $\bar{g}$ is the image of g degraded by the limited aperture.

When the contributions to equation (18) from the other, "accidental" solutions are also included, we obtain

$$\hat{g}(\xi) \simeq \bar{g}(\xi) + \sum_{m} g_m(\xi)$$

where the g_m are the small contributions from any 'accidental' solutions to equation (19).

These considerations suggest that compensation can be obtained during reconstruction in the near-field. There is considerable doubt that compensation can be applied during the recording process, however. Moreover, near-field computer calculations recently carried out suggest that this doubt is justified.

Because the above analysis is not too rigorous, we have supplemented it by computer analysis of the near-field problem. We have taken $y(x) = \alpha x^3$, which is the lowest-order non-trivial array shape. With $x \to m$, $u \to n$ (where m, n are integers), the near-field expressions are taken as:

$$G_n = \sum_{n} g_n \, e^{2\pi i \left[(N+Am^3)^2 + (m-n)^2\right]^{1/2}}$$

$$\hat{g}_n = \sum_{m} G_m \, e^{-2\pi i \left[(N+Am^3)^2 + (m-n)^2\right]^{1/2}}$$

The computer analysis is carried out with the object set $\{g_n\}$ representing a point source at the origin ($g_n = \delta_n$, 0). The parameter values N = 101, m, n = -50, -49, ... +50, $A = 10^{-3}$, correspond to

a severe third-order distortion of the holographic surface, as is shown to scale in Figure 5-3. The reconstruction $\{g_n\}$ given in Figure 5-4 shows that even in this extreme case, the compensation during reconstruction is very effective, even without the amplitude corrections represented by $\cos^2 \theta/\ell$ in equation (30).

5.2.2 Methods of Introducing Shape Compensation

We note from the previous section that, if the Fresnel approximation is valid, the compensation can be provided either during data acquisition or during reconstruction.

The receive gating will always need to be designed to allow for the array shape; this is, of course, necessary whatever compensation method is applied, if any. The compensation during data acquisition may be provided by introducing appropriate phase delays between $\pm$180 degrees in the reference signal applied to the mixer in each channel. However, this method of compensation is a messy one since it involves a reference connection to each channel instead of the present connection to each board (unless the array shape is cylindrically symmetric, of course).

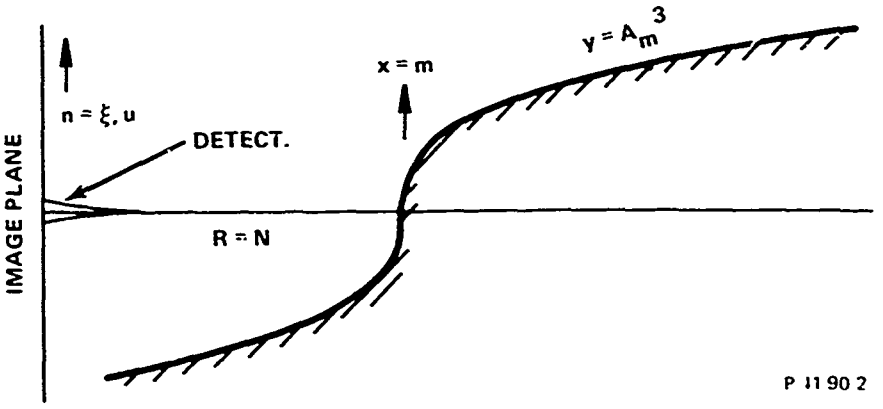

Figure 5-3 - Third-Order Surface Distortion

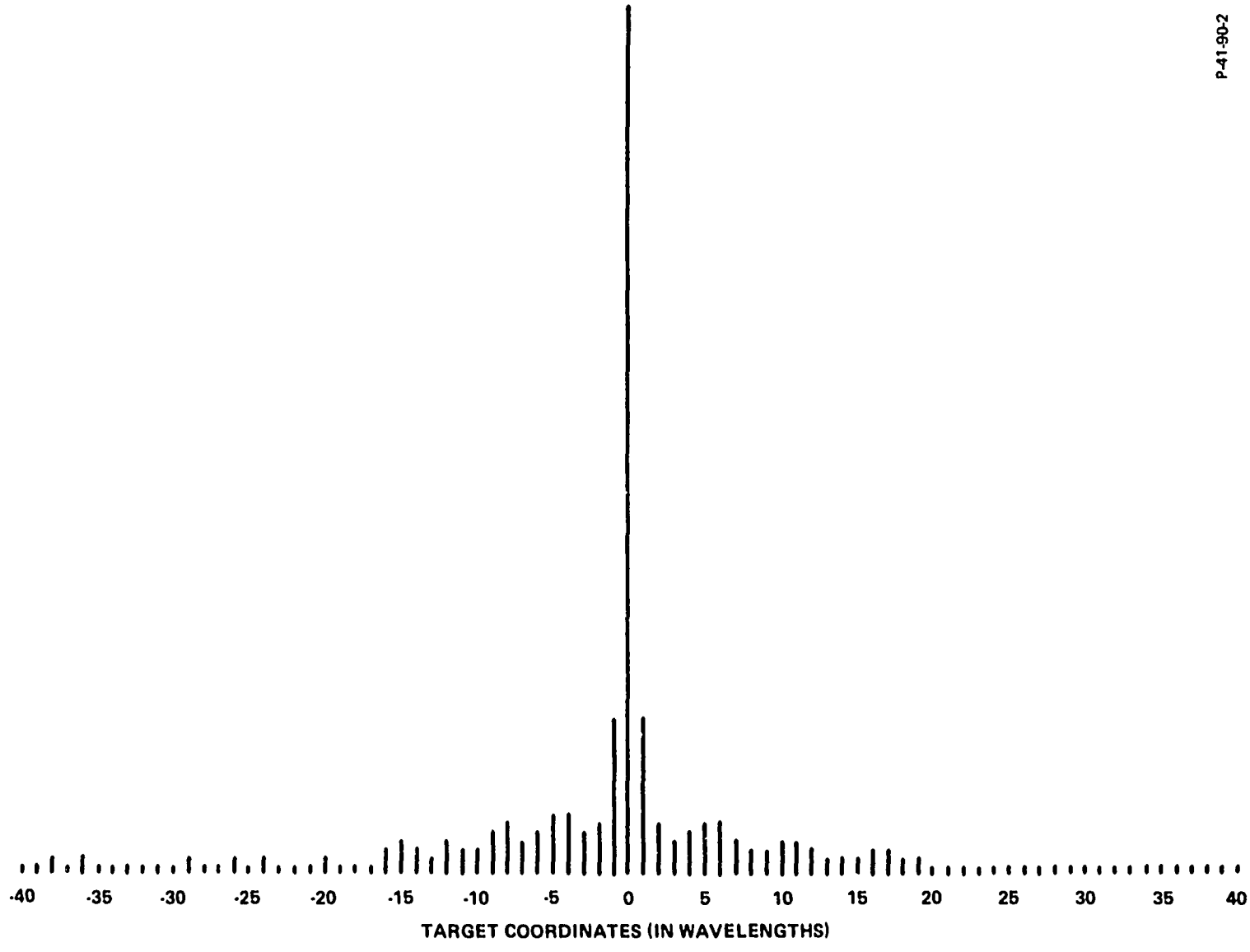

Figure 5-4 - Compensation Results

On the other hand, it does have the advantage of producing stable compensation since it can be carried out digitally. An alternative related approach is to introduce the phase delays in the preamplitier channel. However, a separate delay for each of the different channels is less attractive than the use of reference signal delays.

If both cosine and sine information are being acquired and the latter is being interpolated, then a small special-purpose computer is already available and can be used to provide phase-delays on the sequential data before it is fed to the reconstructor:

$$\cos(\phi + \phi_1) = \cos\phi \cos\phi_1 - \sin\phi \sin\phi_1$$

$$\sin(\phi + \phi_1) = \cos\phi \sin\phi_1 + \sin\phi \cos\phi_1$$

This would require only a maximum of a 2N-word read-only memory (for $\cos\phi_1$, $\sin\phi_1$) and a very simple arithmetic section. If computer reconstruction is being used, there is, of course, no difficulty in producing the necessary phase compensation by this method.

Finally, the phase compensation can be produced at the reconstructor by analog phase delays on the optical beam. This might be achieved by one of three methods: (i) a suitably-shaped optical component placed at the reconstructor tube face, (ii) modifications of the optical phase by additional voltages, and (iii) modification of the digital scan circuitry to allow changes in the position of the written elements to simulate the appropriate phase changes (as in computer-generated binary holograms, for example). Because of difficulties in making complex surfaces to a fraction of an optical wavelength tolerance,

the first approach will not be too easy. The second method involves voltages large enough to produce phase shifts of $\pm\pi$ and is not entirely straightforward. The third method is promising, but the overall effect of this type of compensation has not yet been established. However, it appears that, if the hologram is recorded with the equivalent of an off-axis reference and the image is small compared with the hologram (as is usual), then excellent simulation of phase shifts can be obtained by shifts in the positions of the elements. However, large position changes are required to obtain large phase-shifts and problems with element overlap can occur. (These can probably be solved, however.)

In summary, a number of methods of producing the array shape compensation are available. The most promising approach is the use of small digital computer to produce the required phase shifts. The most promising analog method is probably via position shift during the writing of the hologram. This will also allow stable compensation since the scan circuits are digitally driven.

5.3 REFERENCES

1. First Interim Report, Bendix Report No. 4601 - August 1968.
2. G. G. Goetz, R. F. Koppelmann, and R. K. Mueller, "Real-Time Optical Reconstruction and Display of Acoustic Holograms for an Underwater Viewing System," presented at the Electro-Optical Systems Design Conference/1971 East, New York, New York (September 14-16, 1971).

3. Interim Technical Report, Bendix Report No. 5406, January 1971.

4. G. G. Goetz, "Real-Time Holographic Reconstruction by Electro-Optic Modulation," Appl. Phys. Letters, 17, 2 (15 July 1970).

5. A. W. Lohmann and D. P. Paris, Appl. Opt. 6, 1739 (1967).

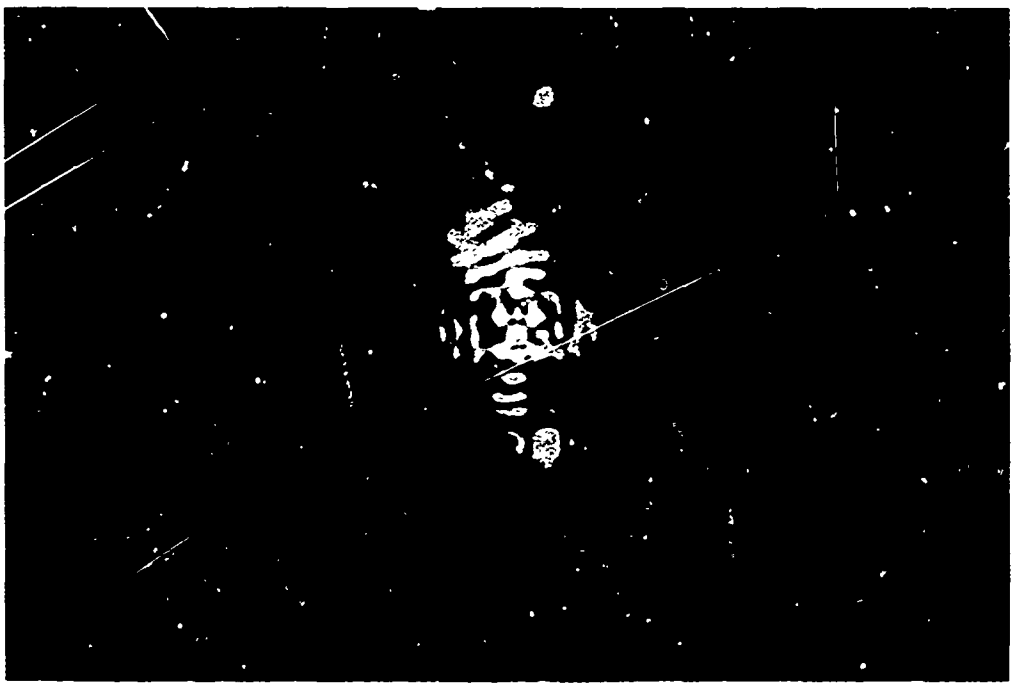

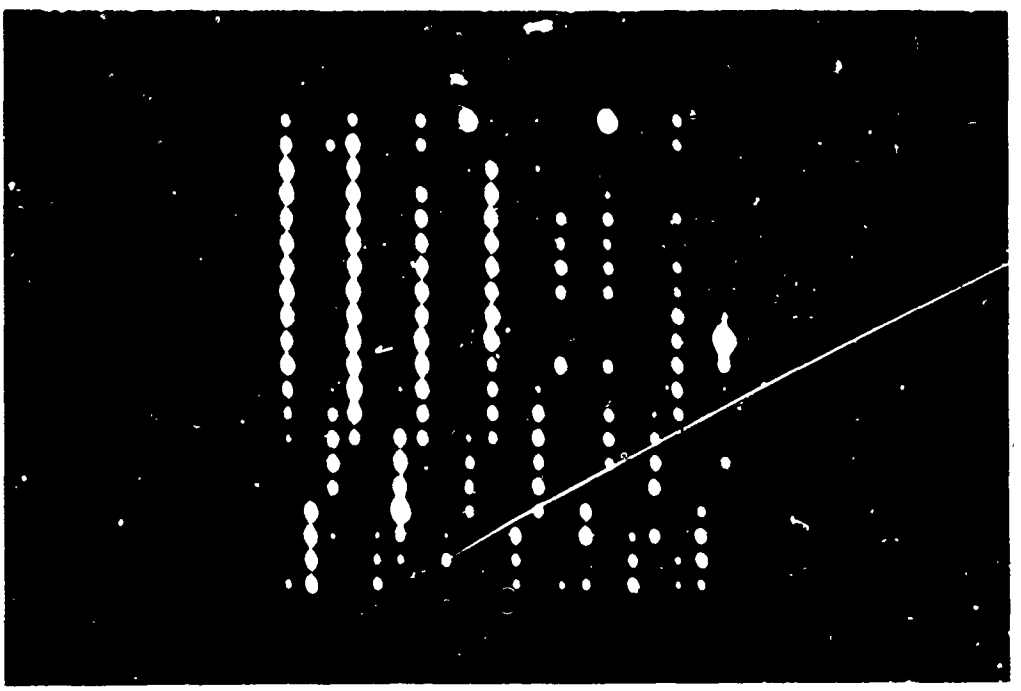

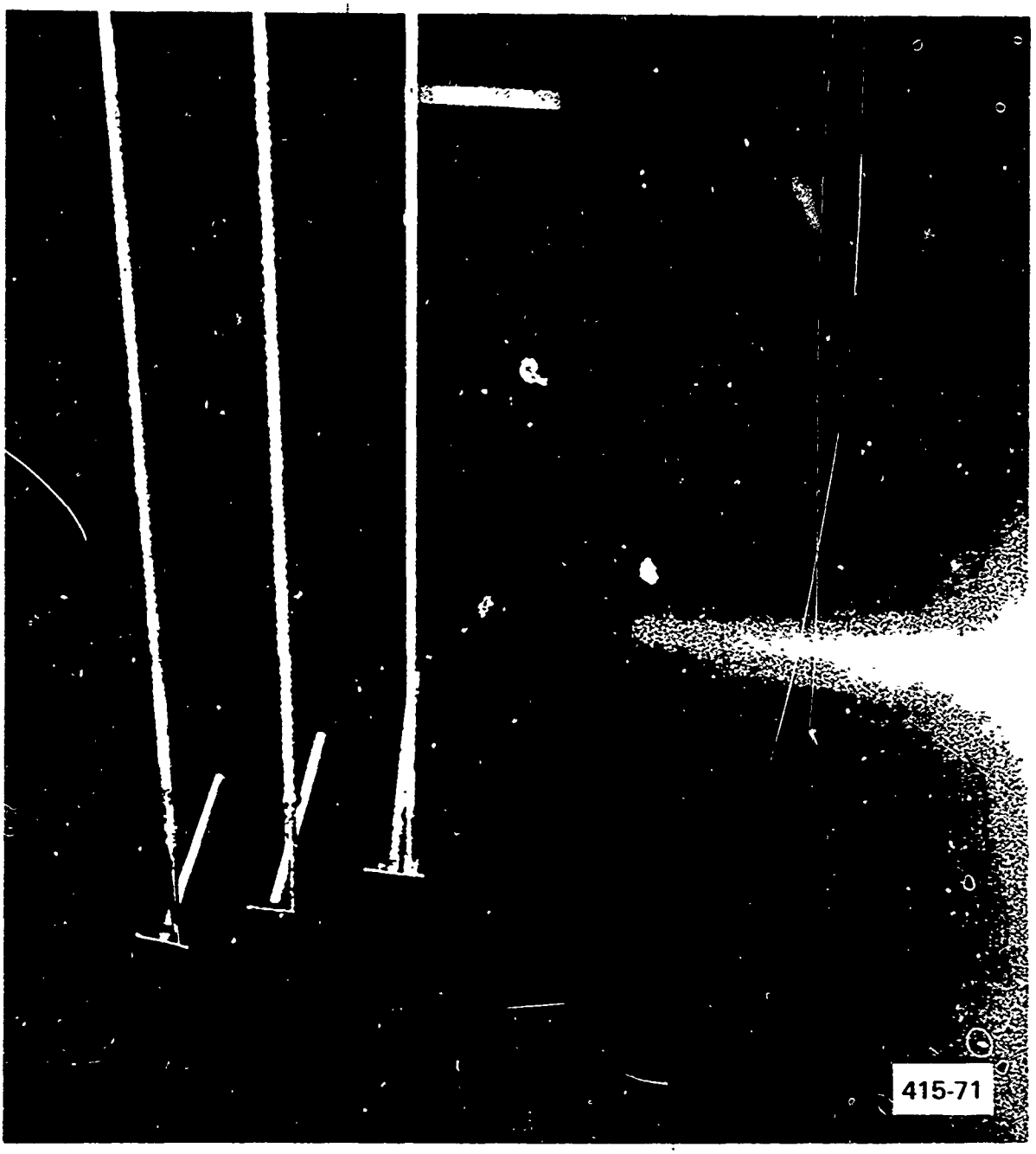
415-71

UNDERWATER ACOUSTIC HOLOGRAM AND ITS RECONSTRUCTION

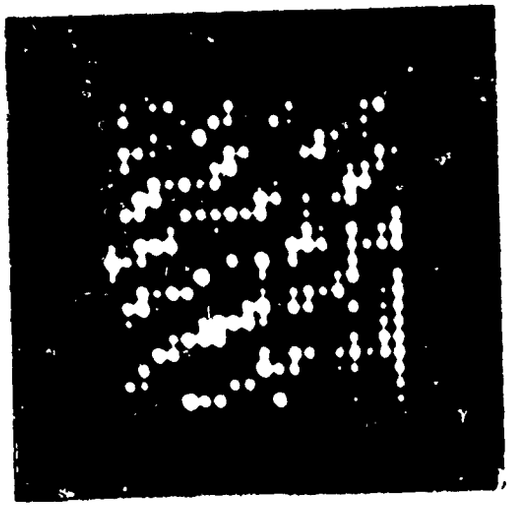

(a) – Underwater Acoustic Holograms of 3 Discs Taken by 20 x 20 Transducer Array

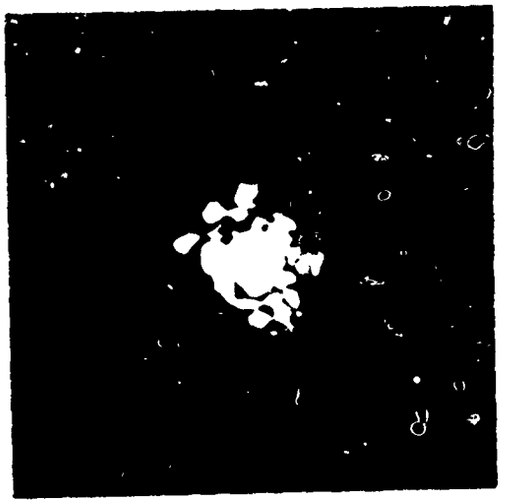

(b) – Reconstruction with DKDP Light Modulator

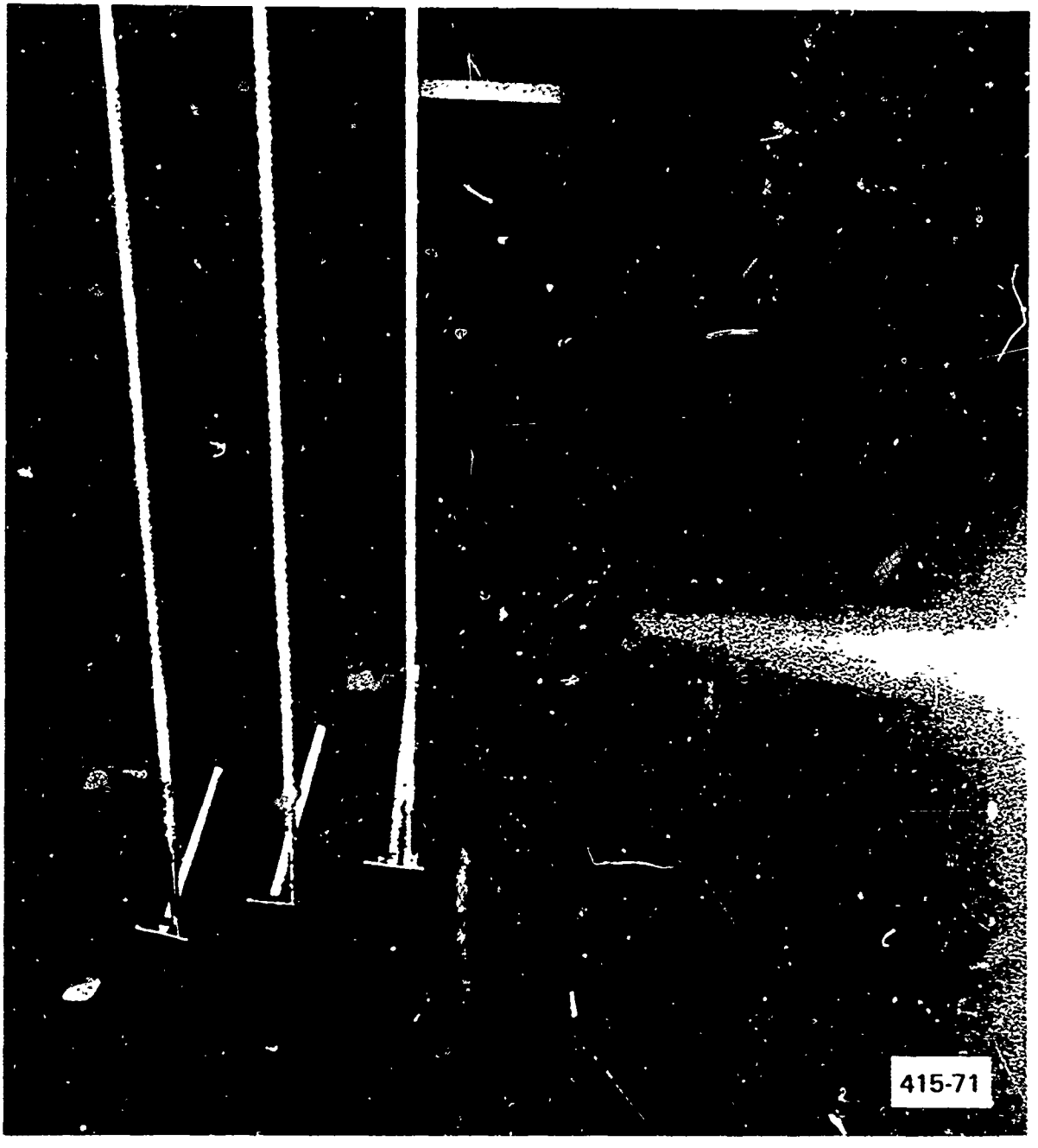
415-71

270-72
10 MM
68 MM
1ST ORDER
DIFFRACTION

τ = 200 μsec

A

τ = 300 μsec

B

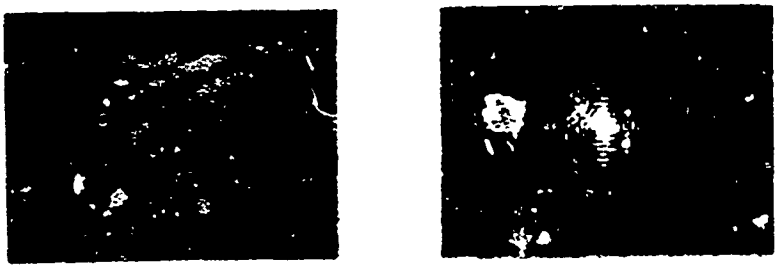

τ = 400 μsec

C

τ = 500 μsec

D

P-41-90-2

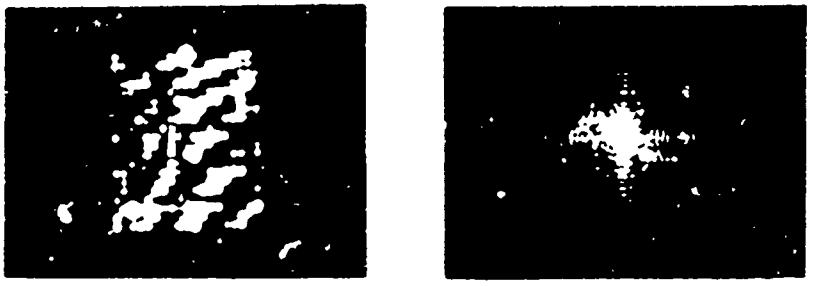

τ = 600 μsec

E

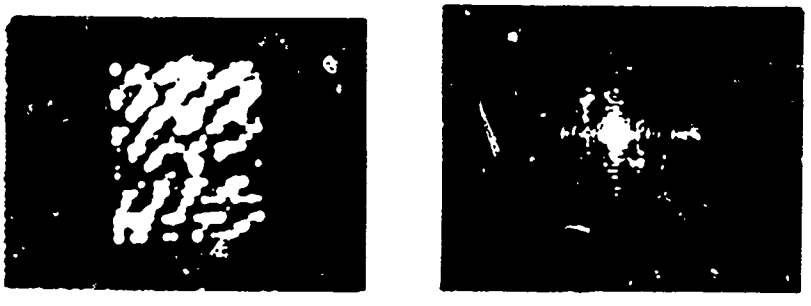

τ = 700 μsec

F

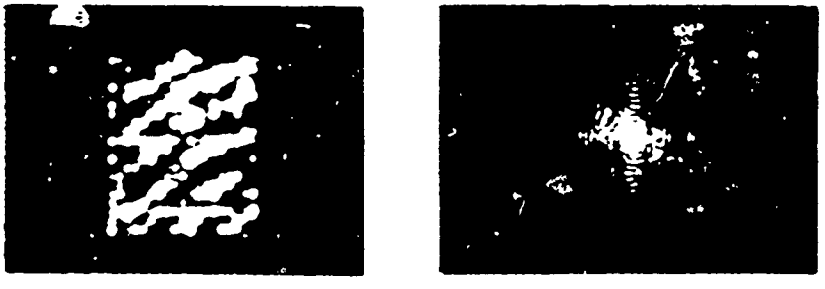

τ = 800 μsec

G

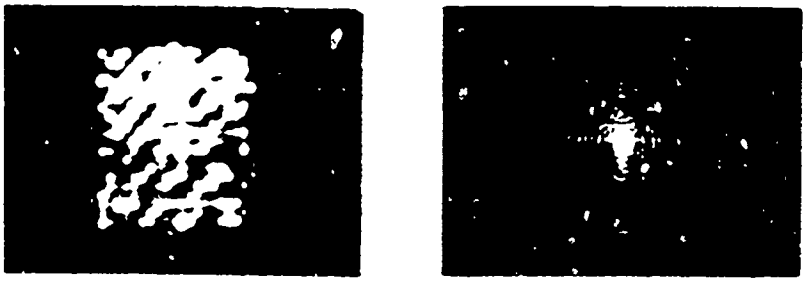

τ = 900 μsec

H

P-41-90-2

τ = 1,000 μsec

I

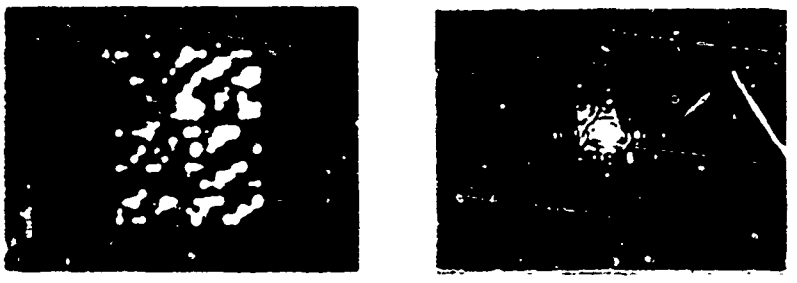

τ = 1,100 μsec

J

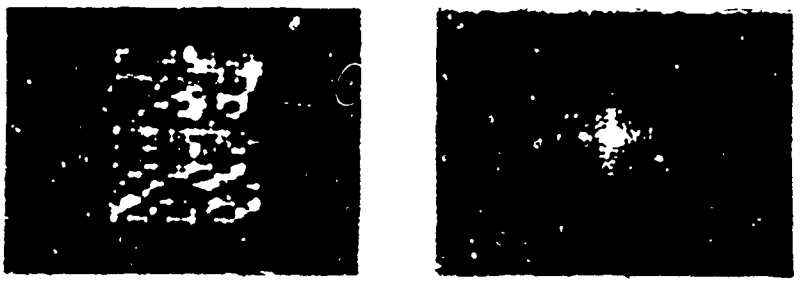

τ = 1,200 μsec

K

P-41-90-2